ELSEVIER

Catena 25 (1995) 269–314

CATENA

The De Ploey erosional susceptibility model for catchments, E_S

Jan De Ploey [a,1], Jan Moeyersons [b], Dirk Goossens [a]

[a] *Laboratory for Experimental Geomorphology, Katholieke Universiteit Leuven, Redingenstraat 16 bis, B-3000 Leuven, Belgium*

[b] *Royal Museum of Central Africa, B-3080 Tervuren, Belgium*

Received 29 December 1993; accepted 30 December 1993

Abstract

This article is based on an unpublished manuscript by the late Prof. Dr. Jan De Ploey. It focusses on the erosional susceptibility of catchments in terms of total energy input by the meteorological factors water and wind (E_S-model).

The form and the universal character of the basic expression of the erosional susceptibility are explained. Applications of the model are illustrated for different processes such as landsliding and debris flows, gullying, creep, and rill–interrill combinations. Characteristic E_S-values exist for these processes. Also, E_S-values vary in regions with differing pedo-botanical characteristics and land-use. The difference between E_S-values for single storm events and longer periods are related to the magnitude–frequency distribution of erosive activities and allow in many cases an assessment of the age of erosion phenomena and an estimation of the recurrence period of extreme single events.

(J.M. & D.G.)

1. Introduction

Never before in history have industrialized and third world countries been more confronted with environmental problems than today. Water management, soil degradation and erosion are becoming a major concern in many parts of the world. For practical and academic purposes an increasing number of laboratories and institutions are interested in adequate prediction, or postdiction, of erosion and ablation rates, especially at the scale of slopes and catchments forming a hydrological unit.

[1] Deceased.

0341-8162/95/$09.50
SSDI 0341-8162(95)00014-3

Many present-day efforts go in the direction of a process-based soil erosion model, a necessary tool in environmental management planning. One of the predecessors of such model was certainly the Universal Soil Loss Equation. Another, more recent model, is WEPP (Nearing et al., 1989), an integration of sediment (continuity) equations for predicting detachment, transport and deposition.

This article presents a model of erosional susceptibility (E_S) for catchments, expressed by the quantity of removed sediment divided by the energy input by water and air. It is a more holistic approach to the complex nature of erosion in drainage basins. Its empirical nature is an advantage because it allows a black box type prediction of the outcome of all possible process combinations to erosion and to sedimentation, both in a short-term and long-term perspective. Furthermore, if the erosional effects of different types of processes can be distinguished, the relative efficiency of these processes can be compared on an objective base.

Prof. Dr. Jan De Ploey, who died in the midst of a very creative phase of his life, devoted his final years to the further elaboration and possible applications of this E_S-model (De Ploey, 1990, De Ploey, 1991a). At the De Ploey Memorial Symposium, which was held in Leuven in March 1993, it turned out that he had left behind an unfinished, but rather detailed manuscript focussing on this topic. Since this manuscript contained a lot of information with respect to the possible applications of the E_S-model in the domains of soil erosion and landscape development, and also as a tribute to Jan, we (J.M. and D.G.) decided to edit the paper and to prepare it for publication.

Many parts of the manuscript have been reworked and reorganised. Although it was thought necessary to make some "corrections", care has been taken to respect the ideas behind every sentence, every word. From this point of view, it was also judged honest to leave the elaboration of the missing sections on sheet erosion, wind erosion and special applications for another occasion. This explains why at some places in the article allusion is made to sheet erosion and wind erosion although these processes are not treated in a separate section.

One important point, treated neither in former E_S publications nor in the original manuscript, is some explanation of the conceptual, or "philosophical", background that led to the elaboration of the E_S-model. Therefore, it was decided to insert in this article the ideas of Jan De Ploey on this topic, expanded in discussions with some of his staff members.

To clarify when and where substantial editorial changes and/or additions to the original text of Jan De Ploey appear in the final manuscript, we have printed these editorial parts in a somewhat smaller font. The contents of these parts are the responsibility of the preparing authors. The list of symbols was also prepared by J.M. and D.G.

(J.M. & D.G.)

2. The E_S erosional susceptibility model

2.1. The form of the basic expression

Inspiration for the erosional susceptibility model for slopes and catchments came from the elaboration of a headcut retreat model for rills and gullies which includes both components of kinetic and potential energy (De Ploey, 1989). The total volume V_T ($V_T = D \cdot w \cdot h$; D = the distance of upstream retreat of the headcut; w = the width of the headcut; h = the height of the headcut) eroded during a period of time t corresponds to

$$V_T = E_r \cdot Q \cdot t \cdot (g \cdot h + u^2/2) \quad (1)$$

where E_r = an erodibility coefficient (units: s^2/m^2), dependent on the local pedo-botanical conditions and the related mechanical properties of the material; Q = total discharge of the flow causing plunge-pool erosion; g = acceleration due to gravity; u = mean velocity with which the flow reaches the headcut.

E_r is, by definition, an empirical "black box" coefficient for which numerical values are obtained by solving Eq. (1) for E_r. The E_S coefficient that is proposed for slopes and catchments has a similar meaning. The factors $g \cdot h$ and $u^2/2$ are expressions of the potential and kinetic energy involved in the headcut retreat event. Matched to flume experiments on headcut retreat in loess loam material, (1) seems to predict V_T values well (Tijskens, 1988).

A parallel approach leads to the following general expression of the erosional susceptibility coefficient E_S for slopes, subcatchments and complete catchments or watersheds which constitute a hydrological unit (De Ploey, 1990):

$$E_S = \frac{V_E}{A \cdot P \cdot g \cdot (h \text{ or } R \cdot S/2)} \tag{2}$$

where E_S = erosional susceptibility coefficient (s^2/m^2); V_E = total soil volume (m^3) eroded within a surface area A (m^2). V_E refers only to erosion that caused ablation, thus a lowering of surface topography. It is related to the rate of denudation; A = the planimetric size (m^2) of the considered area which represents a hydrological unit. There is no limit as to the maximum extension of A. The minimum size will be that of a slope section which can be considered as a hydrological unit (often such a unit will extend from the crest line down to a thalweg); P = total volume of water precipitated per m^2 during a storm event or during any period of time t. Also, $P = p_t \cdot t$, with p_t = total precipitation/m^2 · unit of time (t) and $V_p = A \cdot P = A \cdot p_t \cdot t$ (P and p_t are expressed in m); g = acceleration due to gravity; h = the elevation head loss (expressed in m), corresponding to the mean depth over which V_E was removed. In case of rills (R), gullies (G), landslides and/or debris flows (L, DF), h corresponds to the average depth of those features. In case of soil creep (C) or congelifluxion (CF), h refers to the average depth of the moving soil or debris mantle and its value should not be confused with the average depth of denudation h_a that was realized over an area A_E ($h_a = V_E/A_E$); $R \cdot S$ = the product, in case of sheet flow (SH), of R, an expression of the hydraulic radius (depth) of overland flow, and S, the considered representative slope gradient for a slope or a catchment. The product $R \cdot S$ has the dimension of a length (m). The term $g \cdot R \cdot S/2$ equals $u_0^2/2$, where u_0 = the flow shear velocity and u_0^2 is proportional to the flow shear stress.

Finally, manipulation of E_S refers to two basic expressions:

(a) For landslides and debris flows (L, DF), gullying (G), creep (C), congelifluxion (CF) and rill–interrill wash (R–IR):

$$E_{S\text{-}i} = \frac{V_i}{A \cdot P \cdot g \cdot h_i} \tag{3}$$

where i stands for L, DF, G, C, CF, or R–IR.

(b) For sheet erosion (SH):

$$E_{S-SH} = \frac{2V_{SH}}{a \cdot P \cdot g \cdot R \cdot S} \tag{4}$$

Expression (4) can be adapted to sheet wash (SH) and wind erosion (W) by introducing the factor u_0, the average shear velocity of water or wind, eroding during a considered period of time t:

$$E_{S-i} = \frac{V_i}{A \cdot u_0 \cdot t \cdot g \cdot (u_0^2/g)} = \frac{V_i}{A \cdot t \cdot u_0^3} \tag{5}$$

where i stands for SH or W, $A \cdot u_0 \cdot t$ is a measure of the total water or air mass that passed over A during t, and u_0^3/g is proportional to the transporting capacity of water or wind.

2.2. Significance of the model

2.2.1. A universal operational mode for all erosion processes

The choice of the headcut retreat model as a starting point of the E_S-model and the use of the headcut retreat equation as the basic equation from which all the other equations are derived, is fundamental. It is based upon the idea that many, if not all, erosion processes, looking at first sight quite different, have a single and universal, rather simple, operational mode in common: the retreat of an erosion border, usually a topographic "cliff", in the top layer of the soil. This is the case in gully erosion, mass movement, rill erosion, interrill erosion, sheet erosion, wind erosion and even glacial erosion and river erosion. The elevation of this "cliff" might be large (for example headcut erosion) or small (for example sheet erosion); the cliff may be spatially continuous (for example sheet erosion) or discontinuous (for example splash erosion); it may remain a rather local phenomenon (rill erosion) or may extend over large areas (for example areal wind erosion in the desert); the cliff may retreat quickly (for example a landslide) or extremely slowly (for example in highly resistant rocks). From this point of view, there are no conceptual differences between the erosion of a sand sheet by wind, the erosion of a cultivated field by the retreat of water-formed gullies or the erosion of a slope by landslides. The subprocesses that play a role are, of course, different, and the intensity and the velocity of the process(es) may largely differ. Also, the input factors, and even the mean force that initiates or maintains the erosion, may be quite different (pressure forces and impact forces for wind erosion, gravitational forces for landslide erosion, etc.). However, the main operational mode of erosion remains identical for all these cases: the soil erodes because of the retreat of a topographical erosion cliff. This may be seen as the major conceptual significance of the E_S-model.

From the discussion above, it becomes clear why the headcut retreat equation serves as the initial equation on which all other equations are based.

(J.M. & D.G.)

2.2.2. Erosion as a function of energy input

In the basic expressions (3), (4) and (5), E_S is expressed in s^2/m^2. If both the numerator and the denominator are multiplied by mass, then E_S is expressed as

$$\frac{\text{mass (eroded sediment)}}{\text{mass (rain water)} \cdot (m^2/s^2)} \tag{2''}$$

which means eroded mass (of soil)/input of energy or geomorphic work. In fact, E_S is an expression of the efficiency of geomorphic work, applied to slopes or catchments, resulting in erosion. Low numerator values (V_E), combined with high denominator values, express low erosional susceptibility.

In the case of sheet flow, the denominator in (2″) stands for mass of rain water, multiplied by $g \cdot R \cdot S/2$ (4), and is one relevant expression for the kinetic energy involved in catchment erosion. For the other group of processes, referred to in (3), the denominator in (2″) stands for mass of rain water, multiplied by $g \cdot h$, an expression for an amount of potential energy.

Generally speaking, the denominator in the E_S equation can be considered as an expression of the maximum amount of energy that could be involved in erosion within an area A and during a period of time t. The term "maximum", in the case of erosion by water and/or mass movements, refers to the total amount of precipitation $P = p_t \cdot t$, that enters the E_S expression together with the gravitational acceleration g. The numerator values V_E and A_E are an expression of the geomorphic work, done within the spatial–temporal units A and t.

The transition from (3), (4) or (5) to (2″), although dimensionally sound, needs a numerical correction: V_i in (3), V_{SH} in (4) or V_i in (5) has to be multiplied by the mean bulk density of the eroded sediment (ρ_s) to obtain units of mass, while V_P ($= A \cdot P$) in (3) or (4), or the volume of water passing over A ($A \cdot u_0 \cdot t$) in (5) in the case of water flow, has to be multiplied by the mass density of water to obtain units of mass in the denominator of (2″). Therefore, in the case of energy input by water, (3), (4) and (5) are numerically equal to:

$$\frac{(2'')}{\rho_s}$$

Furthermore, the denominator in (2″) is not expressed in Joules but in kiloJoules, since the precipitation water volume in (3) and (4), or, in case of water flow, the water passing over A in (5), is expressed in m^3, i.e. in units of 1,000 kg mass.

In numerical examples in former publications (De Ploey, 1989, De Ploey, 1991b), the volume of eroded sediment V_E in the numerator of Eq. (3), or V_{SH} in the numerator of Eq. (4), was never transformed into mass. In the same time the volume of precipitated water, V_P, in the denominator of (3) or (4), remained in m^3. In this way the denominator expresses the geomorphic work in kiloJoules. This simple calculation rule has always been applied, but the results were wrongly expressed as kg removed sediment/Joule geomorphic work. In fact, the numerical results have to be expressed in m^3 of removed sediment/kiloJoules of geomorphic work. To put this clear with an example, $E_S = 2 \times 10^{-2}$ s^2/m^2 means that 50 kJ are needed to erode 1 m^3 of sediment.

(J.M. & D.G.)

2.3. *Why introduce the full amount of P?*

It is known from single erosion events that rainfall, water or air flow have to reach a certain threshold in magnitude, duration, intensity or discharge to trigger an erosional process. Therefore, the erosional susceptibility of a catchment will be higher when calculated for a single erosion event than for a longer period, varying from a season to a

geological time span. The latter includes, indeed, a number of energy inputs (for example during rainfall events) with no direct erosional effect for the process considered.

It could be argued that this consideration invalidates the E_S-model where a proportionality between total energy input and eroded volume is postulated. This is not true, because every energy input will have direct and/or indirect effects. Justification for handling the term $V_P = A \cdot P$, the total volume of water precipitated on a catchment, is that each drop of falling water that reaches the Earth's surface influences, directly or indirectly, present and future erosional susceptibility of A. In fact, each such drop of water enters a hydrological cycle which partly governs the pedobotanical and geo-ecological conditions, which control the system of erosive forces, as opposed to friction and resistance to erosion. The latter relationship is intimately connected to the concept of erosional susceptibility and, therefore, the introduction of full P values is very important. Erosion is not only controlled by the "state" of a catchment during the event. Recent literature clearly demonstrated that erosion has a "memory", as it is largely influenced by antecedent weather conditions and hazards within catchments (e.g. in the Negev desert: Yair, 1974; in loess areas: Govers et al., 1990). A primary factor controlling these antecedent conditions is the full amount of P, as a first order geo-ecological factor. Also, in the case of pure chemical erosion, or combined piping and chemical erosion, the ratio V_E/V_P has to be considered as a primary parameter for defining erosional susceptibility. Moreover, P is nearly the only rainfall term for which reasonable numerical ranges can be proposed when discussing long-term values of E_S related to geological time spans.

In reality, precipitation P reflects complex processes and interactions which have ambivalent effects on the final erosion of slopes as expressed by the parameters V_E and A_E. On the one hand P basically controls, within given geo-ecological conditions, factors of resistance against erosion, related to specific pedobotanical circumstances (ground cover by vegetation, resistant soil horizons ...). On the other hand, P is the driving force behind erosion acting upon the erosivity of flows and eventually lowering shear strengths of material which, therefore, becomes more prone to mass movements.

2.4. The planimetric factor A_E/A

E_S can be calculated by the use of parameters as A_E, A, P, V_E, V_P, h and g, defined earlier. They can be collected in the field by rather simple measurements, if they are not already available in the existing literature. Moreover, they often allow a simplification of the basic expressions (3), (4) and (5). For example, by putting $V_E = A_E \cdot h$, (3) reduces to:

$$E_S = \frac{A_E}{A} \cdot \frac{1}{P \cdot g} \tag{6}$$

Similarly, the planimetric factor A_E/A can be introduced in (4) and (5), and becomes part of the discussion of E_S. This approach has a fundamental geomorphological meaning besides the pragmatic fact that A_E data are often more readily available than information on V_E and h. Indeed, if V_E is unknown, A_E/A can be easily obtained,

especially in the case of well pronounced gullies, rills or landslide marks, by simple photographical interpretation. This can be done by planimetric measurements on aerial photographs or by accurate estimations on slides or photographs of the area under study.

The introduction of the planimetric factor A_E/A leads to interesting considerations. It shows that the erosional susceptibility of two catchments with the same V_E-value can be different. In this case, E_S is higher for the catchment where the erosional forms are less deeply carved out so that their lateral or longitudinal extension is more important. In that sense, and for good reasons, the E_S approach takes into consideration the factor of the areal extension of eroded surfaces as a primary factor in defining the erosional susceptibility of land surfaces. Hitherto, too much emphasis has been put upon the volumetric effects of erosion alone. The E_S approach rehabilitates the fundamental meaning of planimetric effects of erosion (ratio A_E/A) as complementary to volumetric erosion data. For example, a valley, entrenched by a deep thalweg gully is not an absolute indication of high erosional susceptibility of the catchment. It merely expresses the overall tendency to generate rivers on drainage lines where shear stresses and streampower of flows are at a maximum. But the relative increase of A_E/A values is an evident indication of a relative high erosional susceptibility when both slopes and thalweg zones are affected by shallow gullying. Such an evolution culminates where badlands are formed and A_E/A tends to 1.

2.5. The "black box" nature of the E_S expression

The global expression of E_S accounts for all possible process combinations resulting in V_E. For example, in the case of rill formation and gullying, E_S is proportional respectively to the ratios V_R/h_R and V_G/h_G. These ratios depend on a combined effect of hydraulic erosion and mass movements, affecting sidewalls and headcuts, which control the evolution of rills and gullies. Different values of these ratios, with h_R, h_G, A and P remaining constant, reflect different erosional catchment susceptibilities, to be associated with varying resistance against the agents of lateral erosion which determine the relative widening of the features. Lateral erosion, thereby, depends on the type of hydraulic erosion acting on the channel bed and its interactions with mass movement processes, which express the relative instability of sidewalls. The factor h results from direct hydraulic erosion, but it also constitutes a basic parameter of shear stresses and shear strenghts on which depends the definition of a critical h_{cr} for collapsing sidewalls.

In the case of sheet erosion, detachment of sediment is presumed to be independent of any mass movements and expressions (4) and (5) apply. The volumes eroded, V_E, are in this case directly related to a measure of the involved shear velocities and shear stresses of flows (parameters R, S, or u_0).

It thus appears that by its true nature, E_S is a "black box" expression for the erosional susceptibility of complex geomorphological units.

2.6. Short- and long-term E_S calculations

It has been mentioned in Section 2.3 that E_S can be calculated for a single erosion event as well as for a longer period. Therefore, a double E_S approach is proposed which

takes into account the time-dependency of erosion hazards: single storm events (se) and long-term (lt) effects. In case of single storm events, the eroded volumes V_E are related to a volume of water $V_P = A \cdot P$ that precipitated on an area A. In principle the computation of $A \cdot P$ assumes adequate information about the spatial distribution of precipitation. Evidently an undefined amount of precipitation, prior to P, may have prepared slopes for erosional events by changing the ratio shear stress/shear strength. Therefore the linkage V_E–$A \cdot P$ forms part of a conventional definition of short-term erosional susceptibility which formally supposes $V_P = A \cdot P$ at the origin of triggered hazards without considering explicitly possible effects of antecedent precipitation which implicitly are taken into consideration when discussing long-term E_S values. Nevertheless this does not preclude an interpretation of obtained short-term E_S values in the light of some information on antecedent weather conditions.

In case of long-term E_S calculations, expressions (3) and (4) apply unchanged. But now $P = p_t \cdot t$ refers to total precipitation for a period of time that may vary between one season and a geological timespan. E_S then brings implicitly to expression the magnitude–frequency distribution of erosive activities within a given area A. Therefore, long-term E_S values for such an area will evidently be inferior to short-term values since the former ones include sometimes considerable precipitation amounts that did not cause any direct erosion except probably creep or chemical erosion. In fact, P may generate continuously chemical weathering and the development of a weathering mantle of depth h_W. If, in a long-term perspective, for example mass movements remove completely and repeatedly those weathering mantles, then:

$$h_{L,DF} = h_W = W_r \cdot t \tag{7}$$

where W_r corresponds to the average weathering rate and t is the time span (yrs).

Substitution of (7) in (3) and solving for W_r gives:

$$W_r = \frac{V_{L,DF}}{E_{S\text{-}L,DF} \cdot A \cdot P \cdot g \cdot t} = \frac{V_{L,DF}}{E_{S\text{-}L,DF} \cdot A \cdot p_t \cdot t^2 \cdot g} \tag{8}$$

whereby $E_{S\text{-}L,DF}$ is derived from expression (3) and P corresponds to the total estimated precipitation for the whole considered geological timespan t ($P = p_t$ (annual precipitation) $\times$ t (yrs)).

2.7. *The age of erosional features and the minimum recurrence interval of extreme events*

Because $P = p_t \cdot t$, Eqs. (2) to (5) can be solved for t if E_S is known. This can be useful, especially in long-term calculations, to determine the age of erosional features. Furthermore, as far as the ranking of E_S values for certain process combinations can be related to specific geo-ecological conditions, the model offers an opportunity for erosion prediction by solving the basic Eq. (2) for E_S. Thus, as stated above:

$$E_S(\text{lt})/E_S(\text{se}) = B \tag{9}$$

For a given area A, taking into account general expression (6) of E_S, one obtains for (9):

$$\frac{A_E(\mathrm{lt}) \times P(\mathrm{se})}{A_E(\mathrm{se}) \times P(\mathrm{lt})} = B \tag{10}$$

or,

$$A_E(\mathrm{lt})/A_E(\mathrm{se}) = (P(\mathrm{lt}) \times B)/P(\mathrm{se}) \tag{11}$$

whereby $P(\mathrm{lt})$ and $P(\mathrm{se})$ correspond to the amounts of precipitation that caused denudation over surface areas $A_E(\mathrm{lt})$ and $A_E(\mathrm{se})$, respectively during a long period of time $t(\mathrm{lt})$ and during one extreme event $t(\mathrm{se})$. For a given period of time $t(\mathrm{lt})$, corresponding to $P(\mathrm{lt})$, total surface area eroded $A_E(\mathrm{lt})$ can be inferior, superior or equal to $A_E(\mathrm{se})$. In the case of $A_E(\mathrm{lt}) = A_E(\mathrm{se})$, (11) becomes:

$$P(\mathrm{lt}) = P(\mathrm{se})/B \tag{12}$$

and since $P(\mathrm{lt}) = p_t$ (annual precipitation) $\times\, t$ (yrs)

$$t = \frac{P(\mathrm{se})}{B \cdot p_t} \tag{13}$$

If, on the other hand, $A_E(\mathrm{lt})$ differs from $A_E(\mathrm{se})$, (11) becomes:

$$t = \frac{A_E(\mathrm{lt}) \cdot P(\mathrm{se})}{A_E(\mathrm{se}) \cdot B \cdot p_t} \tag{14}$$

Eqs. (13) and (14) express relationships between single events and long-term effects of erosion which are dependent upon the magnitude–frequency distribution of erosion hazards.

For a given area A, the recurrence interval $T(\mathrm{se})$ of an extreme event ($P(\mathrm{se})$, $A_E(\mathrm{se})/A$) has to be equal or superior to the period of time t for which $A_E(\mathrm{lt})/A = A_E(\mathrm{se})/A$; otherwise $A_E(\mathrm{lt})$ should be superior to $A_E(\mathrm{se})$, contrary to the examined condition. Therefore, the minimum recurrence interval (in years) for single extreme events, $T(\mathrm{se})$, can be expressed as:

$$T(\mathrm{se}) = \frac{P(\mathrm{se})}{B \cdot p_t} \tag{15}$$

with p_t corresponding to the average annual amount of precipitation and $P(\mathrm{se})$ equal to total precipitation during the extreme event.

3. A discussion of the main E_S domains

3.1. Landslides (L) and debris flows (DF)

Landslides and debris flows all over the world generally characterize subhumid and humid belts with a pronounced relief: scarps, mountain ranges but also hill-regions underlain by rocks with low consistency like pelitic formations.

3.1.1. Calculation examples for single storm events

According to expressions (2) and (3):

$$E_{S-L,DF} = \frac{V_{L,DF}}{A \cdot P \cdot g \cdot h_{L,DF}} \tag{16}$$

with $V_{L,DF}$ corresponding to the volumes evacuated over an average depth $h_{L,Df}$ along planes of failure or on eroded tracks, with a global effect of ablation. It means that non-affected areas within A (depositional areas, or areas where material was in transit without any measurable change of relief) are not included when defining $A_{L,DF}$ (the total surface area eroded by the considered mass movements). Authors may give direct information on both $V_{L,DF}$ and $h_{L,Df}$, the mean depth over which ablation occurred. Otherwise, for

$$V_{L,DF} = A_{L,DF} \cdot h_{L,DF} \tag{17}$$

Eq. (3) is reduced to

$$E_{S-L,DF} = \frac{A_{L,DF}}{A \cdot P \cdot g} \tag{18}$$

in which the planimetric ratio $A_{L,DF}/A$ becomes a major parameter which can be monitored by field surveys or directly by remote sensing.

Calculated E_S values, expressed in m^3/kJ, refer to data from the literature or from those communicated personally by some investigators. Figs. 1 and 2 represent results for

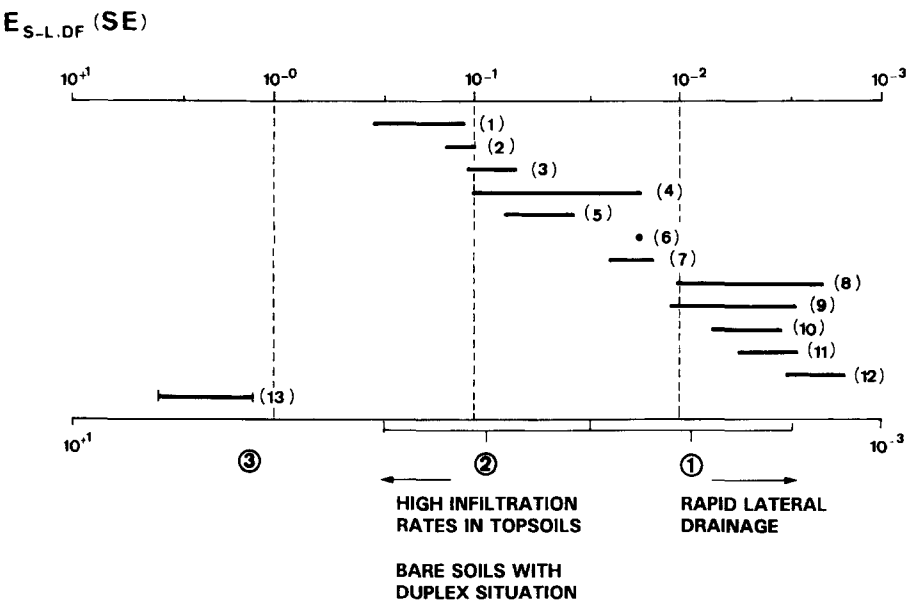

Fig. 1. $E_{S-L,DF}$ domains for single storm events. Numbers in parentheses refer to specific sites described in the text.

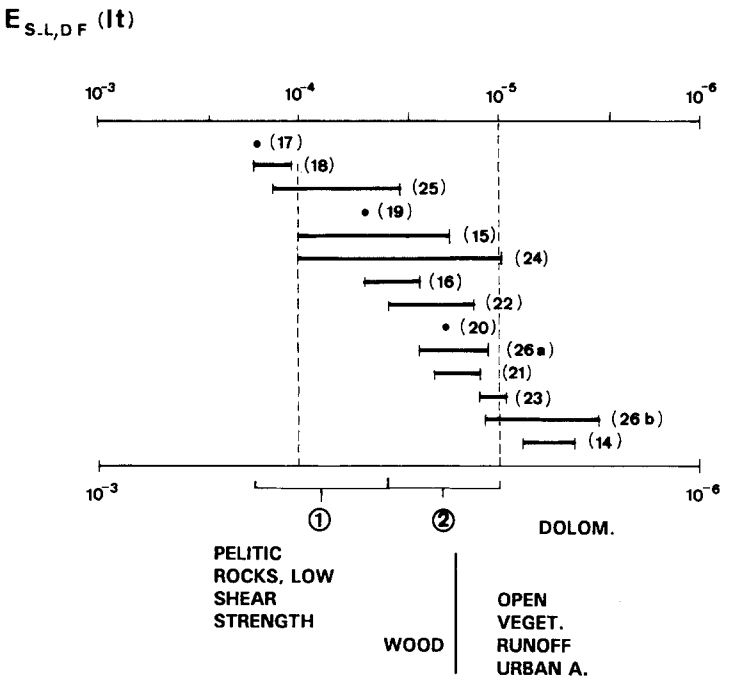

Fig. 2. $E_{S\text{-}L,DF}$ domains for long-term periods. Numbers in parentheses refer to specific sites described in the text.

single storms events and long-term hazards, respectively. Often, authors could not provide precise information on all parameter values entering the $E_{S\text{-}L,DF}$ expression and this was also the case for E_S computations concerning other process combinations. For those parameters, safe maximum numerical intervals were proposed, and this explains why E_S values generally cover a certain range, sometimes close to one order of magnitude.

In many sites earthquakes are and were an important factor for triggering mass movements, and long-term $E_{S\text{-}L,DF}$ computations implicitly include their impact. However, more research is needed to find an adequate expression of seismic energy as part of the E_S equation. Therefore, we left out of discussion single events during which slope failure was exclusively induced by an earthquake of known magnitude.

Below, sites with single storm $E_{S\text{-}L,DF}$ values (see also Fig. 1) are briefly described in order to give some basic information on the geography of the areas concerned.

(1) Ireland (Prior and Douglas, 1971): Landslides and debris flows in August 1970 (P between 0.07 and 0.1 m) on steep cliffs underlain by coarse rubble of angular debris; characteristic bowl-shaped scars. Data clearance for slides Nos. 1, 2, 5 and 6; $E_{S\text{-}L,DF}$ between 1.4×10^{-1} s^2/m^2 and 5.6×10^{-1} s^2/m^2.

(2) Brazil (Jones, 1973): Catastrophic landslides during the January 1967 storm events (P between 0.218 and 0.275 m) in an area between Sao Paulo and Rio de Janeiro underlain by crystalline rocks; steep slopes, S up to 0.9; removal of loamy sandy

weathering mantles varying in thickness between 1 and several m; estimation of A_L/A according to photographs; more slides on forested than on grass-covered slopes! E_S between 1.1×10^{-1} s^2/m^2 and 2.3×10^{-1} s^2/m^2.

(3) Swiss Alps (Kienholz et al., 1991; Haeberli et al., 1989): Effects of heavy rainfall in July 1987 (P estimated between 0.15 and 0.25 m); mass movements related to torrential incisions in steep sloping catchments underlain by crystalline rocks including schists and phyllites; vegetation cover: meadows and forests passing into higher slope sections with periglacial waste deposits. E_S between 8.2×10^{-2} s^2/m^2 and 1.4×10^{-1} s^2/m^2.

(4) Japan (Hiura and Murakimi, 1981): Global evaluation of 90 single storm events for the period 1972–1974 from all over Japan; disasters mainly caused by typhoons or frontal storms in granite mountains with dominant steep forested slopes. Depth of landslides h_L often around 1 m. P estimated between 0.1 and 0.4 m. Authors mention that, in general, A_L/A is inversely proportional to the basin area A which varied between 0.1 and 11 km^2; average $A_L/A = 0.11$. E_S between 2.8×10^{-2} s^2/m^2 and 1.1×10^{-1} s^2/m^2.

(5) Brazil (Cruz, 1974): Disastrous landslides in the coastal Caraguatatuba area during the March 1967 rainstorms totaling about 0.68 m of precipitation; steep sloping "morro's" covered by rain forest; h_L often inferior to 1 m. E_S between 5.9×10^{-2} s^2/m^2 and 8.8×10^{-2} s^2/m^2.

(6) Tanzania (Lundgren and Rapp, 1974): One big bottle slide near Morogoro town in the Uluguru mountains; $P = 0.21$ m; poorly protected cultivated land on cristalline rocks; slope gradient S up to 0.4; removal of clayey soils over a depth h_L of the order of 5 m. $E_S = 2.9 \times 10^{-2}$ s^2/m^2.

(7) California, USA (Ellen and Wieczorek, 1988): Hundreds of landslides/debris flows in the mountainous range south of San Francisco resulting from the January 1982 storms, totalling P between 0.12 and 0.45 m; slope gradients S between 0.6 and 0.7; residential areas, woodland and brush-covered hillslopes underlain by various rock and soil types; A_L/A ratio estimated to range between 0.01 and 0.05. Computation of E_S: between 2.2×10^{-3} s^2/m^2 and 4.2×10^{-2} s^2/m^2.

(8) Southern California (Rice et al., 1969): Numerous soil slippages mapped for the storms of the years 1966 and 1967 in the Bell Canyon watersheds; very steep slopes (S around 0.8) often on gravelous colluvial material; areas with grassland and brush cover; total annual P estimated to 1.2–1.6 m. E_S between 3.6×10^{-3} s^2/m^2 and 1.1×10^{-2} s^2/m^2.

(9) Tanzania (Rapp, 1972): Landslides in the Mgeta area triggered on February 23, 1970; P between 0.1 and 0.185 m; S mainly between 0.35 and 0.85; removal of regoliths mainly on cristalline rocks, with h_L around 1.0–1.5 m; more than 1.000 slides originated in cultivated fields and in grassland, but less than 1% in woodland covered areas. E_S between 4.9×10^{-3} s^2/m^2 and 1.4×10^{-2} s^2/m^2.

(10) Pennsylvania, USA (Pomeroy, 1980): Slides, slumps and debris flows due to July 1977 rainstorms in the Johnstown area (Appalachians); P around 0.3 m; S between 0.35 and 0.85; often elongated erosion scars formed on forested and grassy slopes, with a majority underlain by clayey colluvial material. E_S between 5.5×10^{-3} s^2/m^2 and 8.3×10^{-3} s^2/m^2.

(11) New Zealand (Selby, 1982): Slides and debris avalanches in the Mangawhara Valley after the February 1966 rainstorm event, with P varying between 0.15 and 0.23 m. S around 0.6; slopes covered by pasture grasses and removal of clayey or sandy material including volcanic ashes; h_L inferior to 1 m. E_S between 4.8×10^{-3} s^2/m^2 and 7.4×10^{-3} s^2/m^2. (12) Swedish Lappland and Spitsbergen (Rapp, 1974): Storms of July 1972 on steep mountains slopes covered by coarse debris (Lappland) or underlain by a permafrost table (Spitsbergen); h_L varying between 0.6 m and 2–4 m. E_S between 2.6×10^{-3} s^2/m^2 and 5.3×10^{-3} s^2/m^2.

(13) Quebec, Canada (Bentley and Smalley, 1984): The computation concerns the huge St. Jean Vianney slide which occurred on 4 May 1971, with $P = 0.0185$ m following a period of heavy rainfall and thaw. The slide developed in very sensitive marine clays on a slope $S = 1.0$; residual angle of internal friction was about 5 degrees, so very low as it happens to be for very clayey deposits including quick clays. E_S between 2 and 6.2 but these are rather maximum values because A, the size of the contributing watershed, was difficult to derive from the report and was probably slightly underestimated.

Two examples may illustrate the type of computations based upon expressions (6) and (16).

Brazil (Jones, 1973):

$$E_{S\text{-}L,DF} = \frac{A_L/A = 0.3 \text{ to } 0.5}{(P = 0.218 \text{ to } 0.275\,\text{m}) \times (g = 10\,\text{m/s}^2)}$$

$$= 1.1 \times 10^{-1} \text{ to } 2.3 \times 10^{-1}\ s^2/m^2$$

California (Rice et al., 1969):

$$E_{S\text{-}L,DF} = \frac{V_{L,DF} = 199 \text{ to } 492\,m^3}{(A = 104\,m^2)\,x\,(P = 1.2 \text{ to } 1.6\,m)\,x\,(g = 10\,m/s^2)\,x\,(h_L = 0.35\,m)}$$

$$= 3.6 \times 10^{-3} s^2/m^2 \text{ to } 1.1 \times 10^{-2}\ s^2/m^2$$

3.1.2. $E_{S\text{-}L,DF}$ domains for single storm events

In most sites mass movements were generated by one or several decimetres of precipitation but there is no evident relationship between the E_S ranking and P. In the two cold areas, Canada and Sweden–Spitsbergen, slides and flows occurred after periods with combined rainfall and thaw. Also, there is no evident relationship between the E_S ranking and the average slope gradient value S. All discussed sites belong to mountain ranges with steep to very steep slopes, often underlain by rather fine textured soil or weathering mantle material (loamy sands to sandy loams with appreciable shear strengths). Texture definitely is a discriminating factor, with impact on $E_{S\text{-}L,DF}$ ranking, when substrates are composed either by very sensitive clays or, in the opposite case, by coarse macroporous material with high hydraulic conductivity. It all has to do with the probability of a dramatic decrease of shear strengths within a given geological unit or at the base of a macroporous unit overlying less pervious material. The latter situation

corresponds to a duplex configuration whereby the position of potential planes of failure relates to depths where oversaturation occurs on top of such units as unweathered bedrock, dense soil horizons or fine textured intercalated layers. A dramatic decrease of shear strenghts is likely to occur in clays of very low consistency (the Canadian site) and on many forested slopes where macroporosity and high infiltration rates characterize the rooting zone in loose material. Forests on steep critical slopes only have a stabilizing effect when root systems penetrate into a competent unit (bedrock, consistent soil horizon) as to immobilize an often thin veneer of loose material.

In accordance with the above discussed principles on the evolution of shear strengths, $E_{S\text{-}L,DF}$ ranking reflects the impact of vegetation and land use. Lower $E_{S\text{-}L,DF}$ values manifestly characterize sites and slopes with low infiltrability and relatively high drainage coefficients. The presence in catchments of cultivated land, open grasslands, open brush-covered slopes or residential areas turns the ratio infiltration/surficial or subsurficial drainage towards lower values whereby erosion by water becomes more likely and slide potentials decrease. But extreme rainfall, eventually combined with high meltwater production in periglacial zones, may generate extensive sheet slides in dense grasslands where rooting zones promote rapid infiltration and oversaturation at limited soil depths.

Finally, taking into consideration the above explained criteria, the following succession of $E_{S\text{-}L,DF}$ domains is proposed. Each domain is marked by a minimum E_S value which is considered safe for a conservative estimation of erosion rates as related to the erosional susceptibility of catchments:

1. $E_{S\text{-}L,DF}$ *between* $5 \times 10^{-3}\ s^2/m^2$ *and* $5 \times 10^{-2}\ s^2/m^2$. Catchments marked by pedobotanical conditions and/or land use systems which favour some rapid lateral drainage of slopes: residential areas, open cropland, open grasslands, brush-covered slopes or a mosaic of these units and forests. Also colluvial slopes and talus slopes underlain by deeply drained coarse material. $E_{S\text{-}L,DF}$ values within this domain are supposed to be inversely proportional to global drainage (runoff) coefficients on slopes, and this principle may help to define sub-domains between $5 \times 10^{-3}\ s^2/m^2$ and $5 \times 10^{-2}\ s^2/m^2$.

2. $E_{S\text{-}L,DF}$ *between* $5 \times 10^{-2}\ s^2/m^2$ *and* $5 \times 10^{-1}\ s^2/m^2$. Forested slopes or slopes characterized by any other type of vegetation (dense grasslands...) which promotes high infiltration rates in topsoils during extreme events. Also bare talus slopes with a duplex situation: coarse rubble of a toplayer superposed on a definitely less pervious bottom-layer. In the case of vegetation-covered slopes it is supposed for this domain that average depth of the rooting zone is inferior to the mean depth of the sensitive unit bearing minimum shear strength when extreme infiltration occurs; for example, the base of a weathering mantle.

3. $E_{S\text{-}L,DF}$ *above* $5 \times 10^{-1}\ s^2/m^2$. Definitely more data are needed to pin-point this domain where E_S values can exceed 1.0. It may include moderately sloping areas underlain by pelitic rocks (clays, marls...) with very low shear strengths.

For a given area, it may be relevant to propose an interpolated $E_{S\text{-}L,DF}$ interval

derived from Fig. 1. In that case it will be indicated to compare its geographic–geomorphological situation with the scenery of the reference sites figuring in the diagram. A preliminary field survey of the area will always guarantee a better interpolation. Such a survey may give information on $h_{L,DF}$ values so that relation (16) can be solved for $V_{L,DF}$.

3.1.3. Long-term $E_{S\text{-}L,DF}$ values

As explained in Section 3.1.1, expressions (16) and (18) also apply to long-term computations of $E_{S\text{-}L,DF}$. Here, the magnitude–frequency distribution of slide and debris flows hazards is taken into account. Geography and data of the considered sites can be summarized as follows:

(14) Dolomites (Cortina D'Ampezzo area), Italy (Panizza, 1990): Evaluation of mapped and dated Holocene landslides, debris flows and falls in a steep sloping Alpine area underlain by dolomites, limestones, clays and marls, with a concentration of hazards on pelitic rocks. We estimated annual p_t during Holocene times at 1.0–1.2 m. $A_{L,DF}/A$ put equal to 0.7–0.8, since about 70%–80% of all mapped catchments were affected by mass movements during about 9,000 yrs. $E_{S\text{-}L,DF}$ between 6.5×10^{-6} s^2/m^2 and 8.9×10^{-6} s^2/m^2.

(15) Wairarupa, East coast of the N. Island, New Zealand (Crozier, 1990, pers. commun.): Period of observations and data collection: 1880–1990; annual pt around 1.4 m; average S between 0.46 and 0.57; average $h_{L,DF} = 0.65$ m. Areas underlain by mudstones, sandstones and colluvial loess or primary loess deposits. Striking sheet-slides on pasture land; within an area of about 2,000 km^2 landslide episodes affected about 100 km^2 every 5–6 yrs. Finally, 5–15% of surface area involved in mass movements. $E_{S\text{-}L,DF}$ between 3.2×10^{-5} s^2/m^2 and 1.0×10^{-4} s^2/m^2.

(16) Adelbert range, Papua New Guinea (Pain and Bowler, 1973): Seismically active mountain range underlain by greywackes, marls, siltstones, sandstones and limestones. Steep forested slopes in a tropical belt with annual P around 3.5 m. The denudation rate is estimated to be about 80–100 cm during the last 1,000 years and 60–70% of this can be attributed to earthquakes. Soils which failed were generally poorly developed with slightly weathered parent rock occurring as little as 40–50 cm below the surface. Dramatic slope failures with complete removal of soils and forest vegetation. $E_{S\text{-}L,DF}$ between 4.6×10^{-5} s^2/m^2 and 7.1×10^{-5} s^2/m^2.

(17) Waipapa River Basin, New Zealand (Dymond and Hicks, 1986): Erosion by water and mass movements in a high (1,000–1,700 m) mountain area of the N. Island with temperate to periglacial climatic conditions. Denudation concentrated on erosion scars with poor vegetation. Mean calculated erosion depth $h_{L,DF}$ in the scars around 1.4 m. $E_{S\text{-}L,DF} = 2.9 \times 10^{-4}$ s^2/m^2.

(18) Darjeeling Himalaya, India (Basu and Ghatowar, 1988): Data collection for the Gish River Basin which is partly forested and partly cultivated land. Effects of monsoon rainstorms (annual P of the order of 12 m!) on steep sloping areas (S between 0.85 and 1.20) ravaged by slides and floods. $E_{S\text{-}L,DF}$ equal to 3.2×10^{-5} s^2/m^2 but between 1.2×10^{-4} s^2/m^2 and 3×10^{-4} s^2/m^2 for the period 1964–1984.

(19) Adriatic coast between Pesaro and Vasto, Italy (Cancelli et al., 1984): Analysis of geological features of landslides along 260 km long coastal cliffs underlain by sands,

conglomerates and "blue clays"; dominantly cultivated land. Historical documentation on landslides for more than 200 years. Data from Table I and from figures. $E_{S\text{-}L,DF} = 7 \times 10^{-5}$ s^2/m^2.

(20) Amahata River Basin near Mt Fuji, Japan (Masamu, 1985): Dominant effects of planar slides on steep slopes underlain by sandstone, mudstone and shales. Annual p_t around 2.2 m, with typhoon rainstorms of very high intensity. Deciduous forests and silviculture with pines and cedars. $E_{S\text{-}L,DF} = 3.5 \times 10^{-5}$ s^2/m^2.

(21) Van Duzen River Basin, N. California, USA (Kelsey, 1980): A steep sloping, rapidly eroding coastal range of northern California which receives between 1.25 and 2.50 m of annual rainfall p_t. Slides, avalanches and debris flows on forested sandstone slopes, grasslands and grass-oak woodlands. Covered period: 1941–1975, with catastrophic events in December 1964. $E_{S\text{-}L,DF}$ between 1.9×10^{-5} s^2/m^2 and 3.8×10^{-5} s^2/m^2.

(22) France, Alps south of Barcelonette (Van Steijn, 1992, pers. commun.): Mass movements, mainly debris flows, on alpine slopes with poor vegetation cover (locally Larix-forests beside alpine grasses and herbs) underlain by sandstones, marls, schists and flysch. Covered period 200–300 yrs (datings after lichonometry and dendrochronology); p_t between 1.0 and 1.5 m; $A_{DF}/A = 0.097 - 0.118$. $E_{S\text{-}DF}$ between 2.1×10^{-5} s^2/m^2 and 5.9×10^{-5} s^2/m^2.

(23) Mt Shasta, N. California, USA (Hupp, 1987): An evaluation of debris flows activity on the stratovolcano Mt Shasta for the last 400 yrs; dating mainly according to dendrogeomorphic evidence. Annual p_t estimated at 1.5 m. $E_{S\text{-}L,DF}$ between 9.7×10^{-6} s^2/m^2 and 1.9×10^{-5} s^2/m^2.

(24) Rwaza Hill, Rwanda (Moeyersons, 1981 and pers. commun.): Measurements on rotational surficial slips and accelerated creep, over a depth of 1–2 m on convex slopes and steep midslope section with very clayey soils on phyllites. Humid tropical climate with annual p_t around 1.0 m. Grassland and Eucalyptus plantations beside scattered fields. $E_{S\text{-}L,DF}$ computations: between 1×10^{-5} s^2/m^2 and 1×10^{-4} s^2/m^2.

(25) Mosel Valley vineyard slopes, Germany (Richter, 1982 and pers. commun.): Measurements on mass movements on vineyards with steep slopes (S between 0.27 and 0.70) underlain by slates, graywackes and stony soils, so dominantly pelitic rocks. Annual p_t around 0.7 m. Slide planes at depths h_L between 0.25 m and 1.0 m. $E_{S\text{-}L,DF}$ between 5.4×10^{-5} s^2/m^2 and 2.1×10^{-4} s^2/m^2.

(26) Catchments in the Volga Basin, USSR (Chasovnikova, 1990): (a) Lesnoy forested basin on sand–clay strata; medium steep slopes; annual p_t around 0.6 m. $E_{S\text{-}L,DF}$ between 1.5×10^{-5} s^2/m^2 and 4.5×10^{-5} s^2/m^2. (b) Yelshanka catchment; mainly cultivated land also on sand–clay strata. Less slide and debris flow activity in this better-drained catchment: $E_{S\text{-}L,DF}$ between 5.4×10^{-6} s^2/m^2 and 1.6×10^{-5} s^2/m^2.

Two examples may illustrate the kind of long-term $E_{S\text{-}L,DF}$ computations.

Dolomites (Panizza, 1990):

$$E_{S\text{-}L,DF} = \frac{A_{L,DF}/A = 0.7\text{–}0.8}{P = p_t \cdot t(1.0\text{–}1.2\,\text{m/y} \times 9{,}000\,\text{yr}) \times g(10\,\text{m/s}^2)}$$

$$= 6.5 \times 10^{-6}\ \text{s}^2/\text{m}^2 \text{ to } 8.9 \times 10^{-6}\ \text{s}^2/\text{m}^2$$

Japan (Masamu, 1985):

$$E_{S-L} = \frac{V_L = 2.83 \times 10^6\ m^3}{A(97 \times 10^6\ m^2) \times P(2.2\ m/yr \times 15\ yr = 33\ m) \times g(10\ m/s^2) \times h_L(2.5\ m)}$$

$$= 3.5 \times 10^{-5}\ s^2/m^2$$

3.1.4. Long-term domains and a general discussion of $E_{S\text{-}L,DF}$

The single storm event $E_{S\text{-}L,DF}$ values are related to the magnitude of the mass movement hazards. Long-term values express the efficiency of geomorphic work related to the magnitude–frequency distribution of hazards. It means that large amounts of precipitation P, that occurred during an historical or even a geological timespan t, did not trigger any mass movements whereas biological activity and weathering continuously proceeded.

Therefore, long-term $E_{S\text{-}L,DF}$ values are about three orders of magnitude less than single storm $E_{S\text{-}L,DF}$ values. For single storms 1×10^{-2} s^2/m^2 is a global minimum figure whereas average minimum long-term $E_{S\text{-}L,DF}$ values are about 1×10^{-5} s^2/m^2. A glance to Fig. 2 shows a striking concentration of long-term values within the domain 1×10^{-5}–1×10^{-4} s^2/m^2, whereas single event values are spread over intervals between 1×10^{-3} s^2/m^2 and more than 1 s^2/m^2. Manifestly some compensatory effects govern the magnitude–frequency distribution of mass movements over long timespans in areas of different geographical configuration, in terms of relief, rock types, vegetation and land use. So there appears an interesting relative concentration of long-term values which might express at a worldwide scale a trend towards unification of the erosional susceptibility of catchments in spite of their apparent geographical diversity.

Looking for a conservative prediction of denudation rates by mass wasting, the following succession of E_S threshold values is proposed:

(1) Above 6×10^{-5} s^2/m^2: sites marked by a variety of landscapes underlain by dominant pelitic rocks (clays, mudstones, schists, slates...). The diagram indicates for sites in New Zealand, Adriatic Coast, Rwanda, Mosel Valley a not surprisingly high erosional susceptibility, explained by relative low shear strengths proper to pelitic material including also clay loams and clayey weathering mantles. An E_S value of 6×10^{-5} s^2/m^2 can be considered as a safe, conservative estimation for this domain No. 1.

(2) Between 1×10^{-5} s^2/m^2 and 6×10^{-5} s^2/m^2: often sites with sandy to loamy soils and weathering mantles on cristalline or psammitic rocks. Within this interval, 4×10^{-5} s^2/m^2 is an appropriate lower threshold for areas with a rather dense vegetation cover: forests, plantations, dense woodlands and grasslands or a combination of these units. Manifestly $E_{S\text{-}L,DF}$ values inferior to 3×10^{-5} s^2/m^2 are more characteristic for better drained catchments with significant runoff coefficients and/or poor vegetation cover (open cropland, open natural or semi-natural vegetation, urbanized areas); for the moment, 1×10^{-5} s^2/m^2 is proposed as a lower E_S limit for those environments. Many more data are needed to refine the subdivision

of the whole domain 1×10^{-5}–6×10^{-5} s^2/m^2, if any further delineation becomes in fact evident.The presence of bare, competent dolomites and limestones outcropping over considerable parts of the Italian Dolomites explains why in this area $E_{S\text{-}L,DF}$ lies below $1 \times 10 - 5$ s^2/m^2.

As already concluded from the single-event $E_{S\text{-}L,DF}$ analysis, no significant correlation can be found between the precipitation P, the slope gradient S and the computed $E_{S\text{-}L,DF}$ values. This can be partly explained by the nature of $E_{S\text{-}L,DF}$ which is expressed under the form of a ratio. On the other hand it becomes clear that major $E_{S\text{-}L,DF}$ differentiation is controlled by vegetation and land use and to a more limited extent also by lithology and soil development.

It has been explained in Section 2.7 that the difference in the E_S(se) and E_S(lt) rankings allows some interesting time considerations. The relationship (15) can be numerically exemplified for the case of mass movements. Suppose a tropical mountain range marked by $p_t = 2.0$ m and an extreme event $P(se) = 0.2$ m causing mass movements on forested slopes, over a surface area $A_{L,DF}$(se). Refering to domain (2), 3×10^{-5} s^2/m^2 can be considered as a conservative average E_S(lt) value whereas 3×10^{-2} s^2/m^2 is supposed to be a representative but conservative E_S(se) value. Thus, the minimum recurrence interval T(se) of the considered extreme event will be: $0.2 \times 1{,}000/2.0 = 100$ yrs. According to relation (12), linked to the condition $A_{L,DF}$(lt) $= A_{L,DF}$(se), P(lt) = 200 m is the total amount of rainfall that matches this condition over a period of time of 100 yrs. One has always to bear in mind that considerable amounts of precipitation during that period of time do not generate mass movements except creep. Furthermore, they continuously contribute to chemical erosion, weathering, eventually progressive changes of pedobotanical conditions, all of these being processes that prepare slopes for landslides and debris flow hazards.

Suppose at a geological timescale a dynamic equilibrium between weathering rate W_r and the ablation rate $V_{L,DF}/A_{L,DF} \cdot t$ so that nearly all slopes of an area A were affected by slides and flows, or $A_{L,DF} = A$. For $P = p_t$ (annual amount of precipitation) $\times t$ (yrs) and taking into account relation (16) this will happen after a period of time:

$$t(A_{L,DF} = A) = \frac{1}{E_{S-L,DF} \cdot p_t \cdot g} \tag{19}$$

Substitution of this expression and $V_{L,DF} = A \cdot h_{L,DF}$ in (8) gives for the average weathering rate:

$$W_r = h_{L,DF} \cdot E_{S-L,DF} \cdot p_t \cdot g \tag{20}$$

Application of these expressions to the above-mentioned mountain range, with $p_t = 2.0$ m and $E_{S\text{-}L,DF} = 3 \times 10^{-5}$ s^2/m^2 (domain 1: dense vegetation cover) gives $t = 1/(3 \times 10^{-5} \times 2.0 \times 10.0) = 1{,}670$ yrs.

After (maximum) 1,670 yrs the whole mountain range was eroded by one cycle of landslides and debris flows. Suppose the locally observed average depth of planes of failure $h_{L,DF}$ to be 0.5–1.0 m. Then $W_r = (0.5\text{–}1.0) \times 3.10^{-5} \times 2.0 \times 10$ m/yr = 0.0003–0.0006 m/yr = 0.3–0.6 mm/yr, a minimum rate of annual weathering as far as 3×10^{-5} s^2/m^2 should be considered as a minimum value of the erosional susceptibility coefficient $E_{S\text{-}L,DF}$.

3.2. Creep (C)

3.2.1. Equation and data

Creep is considered as a continuous process whereby soil material or rocks are moving over an average depth h_C, to which applies a certain velocity profile and a mean creep velocity u_C. Within a certain period of time t, which depends upon P (total precipitation/m^2), ablation results from the final evacuation of a volume V_C. Ablation will take place on convex slopes over a surface area A_C:

$$V_C/A_C = h_a \tag{21}$$

h_a being the average depth of ablation over A_C, whereby $h_a = h_C$. After a long geological period of time with continuous creep h_a can become greater than h_C, which means that the total depth of ablation will become greater than the average depth over which material is creeping on the slopes. Also,

$$V_C = h_C \cdot u_C \cdot t \cdot W \tag{22}$$

whereby u_C corresponds to the average creep velocity over depth h_C, during a period of time t; W, measured along a contour line, is the total width of the cross-section(s) through which creeping material is evacuated. Finally,

$$E_{S-C} = \frac{V_C}{A \cdot P \cdot g \cdot h_C} \tag{23}$$

an expression entirely comparable to $E_{S\text{-}L,DF}$ for landslides and debris flows. $E_{S\text{-}C}$ applies to a surface area A of unlimited extent but minimum dimensions correspond to a full slope which constitutes a hydrological unit. $A = A_C$ in the case of a totally convex slope. $P = p_t$ (annual precipitation) $\times$ t (yrs).

Fig. 3 shows computed $E_{S\text{-}C}$ values derived from data of the literature. Again, certain values cover a relatively broad interval for two reasons:

(1) for some parameters authors propose numerical values within a certain range rather than definite values;

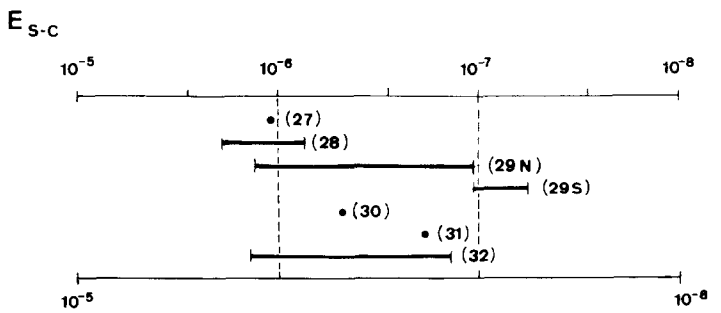

Fig. 3. $E_{S\text{-}C}$ domains. Numbers in parentheses refer to specific sites described in the text.

(2) data were integrated from different sites, e.g. the data of Saunders and Young (1983).

The geography of the discussed sites can be summarized as follows.

(27) Swiss Alps near Aigle (Bonnard, 1983): Thorough analysis of deep creeping; h_C about 50 m. Hummocky fairly steep slopes (S around 0.25) mainly under pastures with movements in flysch. Annual p_t around 1 m. Considered area $A = 2.8$ km^2. $E_{S\text{-}C} = 1.4 \times 10^{-6}$ s^2/m^2, for V_C estimated at 2,000 m^3/yr.

(28) Sudety Mts, S. Poland (Jahn and Cielinska, 1974; Jahn, 1981): Measurements of soil creep on grass covered steep ($S = 0.80$) slopes; $h_C = 0.3$ m; u_C/yr = 0.005–0.015 m; $W = 1$ m; $p_t = 1.5$ m; ablation on convexities with a length varying between 100 m and 1,000 m. $E_{S\text{-}C}$ between 8.8×10^{-7} s^2/m^2 and 3.5×10^{-6} s^2/m^2.

(29) Northern Territory and Southern Tablelands, Australia (Williams, 1973): Soil creep rate measurements on various sandy soils in the northern tropical environment ($p_t = 1.23$ m); podzolic soils in the southern temperate upland ($p_t = 0.8$ m); sclerophyll forests, eucalypt woodland over grasses in catchments with low slope gradients S, between 0.02 and 0.18; $h_C = 0.3$ m; u_C varying between 1.47 mm/yr–2.43 mm/yr in the northern tropical belt, between 0.63 mm/yr and 1.07 mm/yr in the southern temperate upland; $W = 1$ m. Ablation on convexities supposed with a length varying between 100 m and 1,000 m. For 100 m length: $E_{S\text{-}C}$ up to 2.0×10^{-6} s^2/m^2 in the north, up to 1.3×10^{-6} s^2/m^2 in the south. For 1,000 m slope length: $E_{S\text{-}C}$ down to 1.2×10^{-7} s^2/m^2 in the north and 7.9×10^{-8} s^2/m^2 in the south.

(30) Oregon coast range, USA (Dietrich and Dunne, 1978): Analysis of the sediment budget of the 16.2 km^2 Rock Creek basin underlain by volcanic rocks. Denudation depending mainly on dissolution. Creep representing about 30–40% of total denudation; $p_t = 3.4$ m; steep forested convex slopes; $h_C = 1.4$ m, an estimated average value for all creeping soils. Annual denudation by creep, $V_C = 34$ m^3/km^2. $E_{S\text{-}C} = 7.1 \times 10^{-7}$ s^2/m^2.

(31) Somerset, UK (Finlayson, 1981): Slopes (S between 0.022 and 0.55) covered by heath grasses, heather and ling on free draining brown earths. Mean creep rate $u_C = 0.39$ mm/yr, calculated according to data originating from sites 2, 4, 5, 10, 11, 12, 13 and 21, near the $S = 0.36$ contour line; $W = 700$ m; $h_C = 1.0$ m; $p_t = 1.08$ m; $V_C = 0.273$ m^3 for $A = 75{,}000$ m^2. $E_{S\text{-}C} = 3.3 \times 10^{-7}$ s^2/m^2.

(32) Data from 13 sites in temperate, mediterranean and tropical areas (Saunders and Young, 1983): Out of consideration are exceptional high creep rates measured in Oregon and in Central California. A global average $E_{S\text{-}C}$ range is calculated for mainly convex slopes with: $p_t = 1.0$ m; $h_C = 0.25$ m; A between 100 m^2 and 1,000 m^2 ($W = 1.0$ m $\times$ slope length, varying between 100 m and 1,000 m); $E_{S\text{-}C}$ between 2.3×10^{-7} s^2/m^2 and 2.3×10^{-6} s^2/m^2, for $u_C = 2.34$ mm/yr.

Two examples to clarify the $E_{S\text{-}C}$ computations:

Data of Saunders and Young (1983):

$$E_{S-C} = \frac{V_C = 0.000585\,\text{m}^3}{A(100\text{ to }1{,}000\,\text{m}^2) \times p_t(1\,\text{m}) \times g(10\,\text{m/s}^2) \times h_C(0.25\,\text{m})}$$

$$= 2.3 \times 10^{-7}\,\text{s}^2/\text{m}^2 \text{ to } 2.3 \times 10^{-6}\,\text{s}^2/\text{m}^2$$

Swiss Alps (Bonnard, 1983):

$$E_{S-C} = \frac{V_C = 2{,}000\,m^3}{A(2.8 \times 10^6\,m^2) \times p_t(1\,m) \times g(10\,m/s^2) \times h_C(50\,m)}$$
$$= 1.4 \times 10^{-6}\,s^2/m^2$$

3.2.2. Creep domains and a discussion of $E_{S\text{-}C}$ values

Most $E_{S\text{-}C}$ computations apply to convex slopes for which $A = A_C$, with ablation affecting the whole slope length L. But authors seldom gave direct information on slope lengths. Sometimes L could be estimated from published sketch maps of the considered area. In other cases L was thought to have varied within an extreme interval 100–1,000 m. 1,000 m is a rather unrealistic large figure for which $E_{S\text{-}C}$ tends to drop to values around 1×10^{-7} s^2/m^2 since L enters via A the computation of the numerator. Therefore the lower limit of expected $E_{S\text{-}C}$ values is shifted up to 3×10^{-7} s^2/m^2 and the interval from 3×10^{-7} to 2×10^{-6} s^2/m^2 is a safe estimate for $E_{S\text{-}C}$ variance on a worldwide scale.

One might expect increasing $E_{S\text{-}C}$ values, towards 1×10^{-6} s^2/m^2, on convex slopes marked by a pronounced curvature in relation to steep mid-slope portions. Furthermore there are some indications that $E_{S\text{-}C}$ is higher on slopes with poor surficial drainage (forests, grassland). This category may correspond to a subdomain with a lower limit of $E_{S\text{-}C} = 6 \times 10^{-7}$ s^2/m^2. Such an evolution conforms to the one proposed for $E_{S\text{-}L,DF}$. One might also expect relatively higher $E_{S\text{-}C}$ values for slopes underlain by clayey material but no clear conclusion can be drawn on that point from the limited set of analysed data.

Overall h_C seems to vary between 0.25 m and 1.0 m, depths comparable to $h_{L,Df}$ for landslides and debris flows in many areas. For $A = 10^6$ m^2 and a convex slope where $P = p_t$ and $g = 10$ m/s^2 one derives from (23) the annual rate of ablation:

$$V_C = E_{S-C} \cdot A \cdot p_t \cdot g \cdot h_C = (2.5 \times 10^6 \text{ to } 1.0 \times 10^7) \cdot p_t \cdot E_{S-C} \tag{24}$$

For steep-sloping, poorly-drained areas a conservative application of (24), after introduction of $E_{S\text{-}C} = 6 \times 10^{-7}$ s^2/m^2, gives $V_C = (1.5\text{–}6.0) \cdot p_t$, or 1.5–6.0 $m^3/km^2 \cdot yr$ for $p_t = 1$ m, with more precision if field evidence allows for pin-pointing h_C.

For low-sloping or well-drained areas, V_C would be half that value. $E_{S\text{-}C}$ equal to 3×10^{-7} s^2/m^2 can be proposed as a conservative estimation of the erosional susceptibility coefficient in that case.

Interesting is the comparison of $V_{L,DF}$ to V_C, derived from basic relations (16) and (23):

$$V_{L,DF}/V_C = \frac{E_{S-L,DF} \cdot A \cdot P \cdot g \cdot h_{L,DF}}{E_{S-C} \cdot A \cdot P \cdot g \cdot h_C} \tag{25}$$

and for the same area (A,P):

$$V_{L,DF}/V_C = \frac{E_{S-L,DF} \cdot h_{L,DF}}{E_{S-C} \cdot h_C} \tag{26}$$

Since $E_{S\text{-}L,DF}$ values exceed $E_{S\text{-}C}$ by two orders of magnitude ($10^{-5}/10^{-7}$):

$$V_{L,DF} = 100 V_C \cdot h_{L,DF}/h_C \tag{27}$$

$V_{L,DF}$ will be a multiple of $100 \cdot V_C$ if $h_{L,DF}$ is a multiple of h_C, but quite often $h_{L,DF}$ is close to h_C, with creep preparing slopes for landslides and debris flows. Substitution of (21) in (27) and solving for h_a gives:

$$h_a = \frac{V_{L,DF} \cdot h_C}{100 \cdot A_C \cdot h_{L,DF}} \tag{28}$$

and for $A_C = A$ (dominant convex slopes):

$$h_a = \frac{A_{L,DF} \cdot h_C}{100 A} \tag{29}$$

with $A_{L,DF}$ being often easier measured than $V_{L,DF}$.

Of course relations (26) and (27) have to be considered as a first rough approximation of the ratio $V_{L,DF}/V_C$. Future investigations have to clarify the numerical evolution of the ratio $E_{S\text{-}L,DF}/E_{S\text{-}C}$ worldwide for different areas with different geographical–geological conditions. If they would bring out possible opposite tendencies in the evolution of $E_{S\text{-}L,DF}$ and $E_{S\text{-}C}$ then relation (26) will appear much less significant. For example, in case $E_{S\text{-}L,DF}/E_{S\text{-}C} = 10^{-5}/10^{-6}$: $V_{L,DF} = 10 \times (V_C \cdot h_{L,DF}/h_C)$. This rises the interesting question of possible convergent, divergent and even opposite tendencies in the erosional susceptibility of catchments for different types of mass movements such as landslides, debris flows and creep. For the moment, as discussed above, our option favours a convergent evolution of $E_{S\text{-}L,DF}$ and $E_{S\text{-}C}$ advocating that areas with the highest $E_{S\text{-}L,DF}$ values are also characterised by the highest $E_{S\text{-}C}$ values.

3.3. Gullying and badlands

3.3.1. $E_{S\text{-}G}$: definition and data

Ephemeral ravines and gullies in croplands and in areas with a natural or semi-natural vegetation are among the most conspicuous erosional features resulting from process combinations including hydraulic erosion and mass wasting acting on headcuts and sidewalls. In many parts of the world the actual development of thalweg gullies in valley bottoms is very striking but they may also entrench drainage lines of hollows and subcatchments and retreat up to divides. It is still not clearly understood under what conditions gullies bifurcate and evolve into gully systems that tend towards the formation of badlands. This question also arises when the deepening of rills on full slope sections produces a gully network.

Short-term erosion rates in gullies can be obtained from direct monitoring during an observation period. Long-term information on erosion rates may require dating of some original surface which was entrenched since the corresponding period of time t. During t, hydraulic erosion evacuated material over maximum depths h_G along the longitudinal profile of the gully and the same depths h_G controlled the retreat of sidewalls by mass wasting. Therefore h_G enters the $E_{S\text{-}G}$ expression which is fully analogous to $E_{S\text{-}L,DF}$:

$$E_{S-G} = \frac{V_G}{A \cdot P \cdot g \cdot h_G} = \frac{V_G}{A \cdot p_t \cdot t \cdot g \cdot h_G} \tag{30}$$

with V_G being the total volume evacuated by gully erosion within a given surface area A during a period of time t, marked by a total volume of water precipitated $V_p = A \cdot P = A \cdot p_t \cdot t$. The size of A can be of unlimited extent: a slope profile, a subcatchment or a complete stream catchment at up to regional scales. The parameter h_G corresponds to the average maximum depth of all considered gully sections. In the case of dominantly U-shaped gullies,

$$h_G = V_G / A_G \tag{31}$$

with A_G being equal to the total gullied surface within A. In case of V-shaped gullies h_G will come close to $2 \cdot V_G / A_G$. Taking into account (31) there is also a planimetric expression of $E_{S\text{-}G}$:

$$E_{S-G} = \frac{A_G}{A \cdot P \cdot g} \tag{32}$$

Eq. (32) offers interesting perspectives to define $E_{S\text{-}G}$ by teledetection monitoring.

The time scale in expressions (30) and (32) is unlimited. V_G and A_G may refer to a geological timespan, or to a limited period of time during which gully expansion was monitored; it simply refers to a volume $V_G = A_{Gi} - V_{G0}$, measured during a monitoring period $t = t_i - t_0$, with a possible expansion $A_G = A_{Gi} - A_{G0}$.

From the available literature 29 $E_{S\text{-}G}$ values could be derived. In Fig. 4 the data are separated into the tropical and the extra-tropical world. Again, for some sites $E_{S\text{-}G}$ values cover a wide range which is due to the degree of uncertainty of some parameters and figures presented by the authors; in these cases a safe, maximum, interval was taken into consideration.

(33) Papua New Guinea (Ollier and Brown, 1971): Erosion on a volcano that was built up in 1937, consisting of pumice and ash. Development of a radial system of gullies with most intensive erosion during the first years; h_G up to 8 m; annual p_t around 2.2 m; S up to 0.6. $E_{S\text{-}G}$: 7.5×10^{-4} s^2/m^2.

(34) Lesotho (Nordström, 1988): Detailed study of gullying in 8 catchments with piedmont plains and steep (S above 0.2) mountain slopes; mainly cultivated land and degraded grasslands. Incision in hard bedrock (basalts) and in duplex soils with sandy loams and clays (piping). Both V- and U-shaped gullies; p_t between 0.7–0.8 m. $E_{S\text{-}G}$ between 4.8×10^{-5} s^2/m^2 and 1.6×10^{-4} s^2/m^2.

(35) S.E. Brazilian Plateau, Brazil (Coelho Netto et al., 1988): Thalweg gully II developed after the introduction of cattle, after 1870, in trampled tropical grassland. Hilly topography underlain by clay-rich sandy soils on colluvial and alluvial deposits (''rampas''). Annual p_t around 1.5 m; estimated h_G: 10 m. $E_{S\text{-}G}$: 3.6×10^{-5} s^2/m^2.

(36) Nono Valley, NE Nigeria (Van Noten and De Ploey, 1977): Savanna woodland in the Gongola Basin underlain by Precambrian marls and sandstones. Gently undulating topography with vertisols on sandy–clayey alluvial and colluvial deposits. Thalweg gullying started around 1952 when vegetation was fully cleared for cotton cultivation. A_G/A = 1–5 km^2/350 km^2; p_t around 0.7 m. Thalweg gullies evolved downstream into wide, intermittent watercourses, ''mayo's''. $E_{S\text{-}G}$ between 1.6×10^{-5} s^2/m^2 and 8×10^{-5} s^2/m^2.

(37) Safahary Plateau, Madagascar (Rossi and Salomon, 1979): Impressive gully

development ($h_G = 50$ m), so-called "sakasaka", on a sandy piedment plateau in an area where deforestation started 80 yrs ago and vegetation turned into a steppic savanna. A_G estimated after data of Rossi and Salomon's Fig. 4; $p_t = 1.3$ m. $E_{S\text{-}G}$ between 1.1×10^{-5} s^2/m^2 and 3.7×10^{-5} s^2/m^2.

(38) Queensland, Australia (Ciesiolka, 1987): Mainly thalweg gullying in degraded grassed woodland of the Nogoa watershed. Gully headcut retreat during 26 years in duplex soils with loamy sands, sandy loams and clay loams; p_t around 0.735 m. $E_{S\text{-}G}$: 2.9×10^{-5} s^2/m^2.

(39) Imiga watershed, Burkina Faso (Mietton, 1988 and pers. commun.): Flat catchments under savanna woodland in Central Burkina Faso, near Zorgo city, nowadays degraded by intensive cultivation; erosion on ferruginous sandy clay loams with duricrusts; h_G around 1 m; $p_t = 0.56$ m. Measurements of A_G between March 1982 and July 1983. $E_{S\text{-}G} = 2.1 \times 10^{-5}$ s^2/m^2.

(40) Northern Burkina Faso (data of Some, mentioned by Mietton, 1988): Long single gully development in the Subsahelian belt (p_t between 0.4 and 0.6 m), in intensively cultivated steppic woodland with ferruginous loamy sands and duricrusts; h_G between 0.4 and 0.6 m. $E_{S\text{-}G}$ between 2.2×10^{-5} s^2/m^2 and 7.9×10^{-6} s^2/m^2.

(41) N. Tanzania (Murray-Rust, 1972): Analysis of soil erosion and reservoir sedimentation in a grazing area west of Arusha, Kisongo watershed near Monduli Mt. Intensive gullying in a degraded savanna with very clayey vertisols on the footslopes of an extinct volcano. S up to 0.30; $p_t = 0.86$ m. Rates of erosion estimated for the period 1960–70. $E_{S\text{-}G} = 8.9 \times 10^{-6}$ s^2/m^2.

(42) N. Nigeria (Smith, 1982 and pers. commun.): Yashi catchment near Zaria in a degraded savanna with sandy clay loams, laterite cappings and scrub vegetation; $p_t = 1.1$ m. Age of the gully system varies between 1,000 and 1,300 yrs. According to Smith: $A_G/A = 0.05$. Pattern of dentritic gully systems in an area of undulating plains. $E_{S\text{-}G}$ between 3.5×10^{-6} s^2/m^2 and 4.5×10^{-6} s^2/m^2.

(43) Kinshasa, Zaire (De Ploey, unpubl. data, 1963–1968): Sandy hill region in the suburban zone of Kinshasa and gullying on moderate to steep slopes of the Matete Valley which was geomorphologically mapped during the 4 yrs observation period. Degraded savanna grassland partly under cultivation; $h_G = 4$ m; $p_t = 1.3$–1.5 m. $E_{S\text{-}G}$ between 6.0×10^{-6} s^2/m^2 and 6.6×10^{-6} s^2/m^2.

(44) S. Burkina Faso (Mietton, 1988 and pers. commun.): Gullying in a flat savanna area belonging to the Pô Basin. Savanna woodland on ferruginous loamy soils in the southern humid belt; p_t around 0.8–0.9 m. Measurements July 1979–March 1981. $E_{S\text{-}G}$ between 2.6×10^{-6} s^2/m^2 and 3.2×10^{-6} s^2/m^2.

(45) S. Nigeria (Osuji, 1984): Severe gullying related to shifting cultivation in a densely populated rain forest belt of S. Nigeria (State of Imo) underlain by sandy ferrallitic soils; p_t between 2.0 and 2.5 m. S between 0.05 and 0.25. Average h_G: 10–50 m; some gullies reach depths of more than 100 m. $E_{S\text{-}G}$ between 1.2×10^{-6} s^2/m^2 and 7.2×10^{-6} s^2/m^2.

Arid, semi-arid and temperate areas:

(46) Moldavian Tableland, Romania (Ionita, 1986): Cultivated land in the Gheltag Basin; loamy sandy to loamy clayey grey forest soils in an area with $p_t = 0.45$–0.6 m; $A_G/A = 0.004$. $E_{S\text{-}G}$ between 6.7×10^{-5} s^2/m^2 and 8.9×10^{-5} s^2/m^2.

(47) N. California, USA (Kelsey, 1980): Sediment budget and quantitative analysis of geomorphic processes in the humid Van Duzen River Basin; $p_t = 1.85$ m; steep slopes. Data 1941–1975 include catastrophic effects of rainstorms in December 1964. Shallow gullying in grasslands; h_G between 1.0 and 3.0 m. V_G derived from analysis of fluvial sediment yield from hillslopes. $E_{S\text{-}G}$ between 2.9×10^{-5} s^2/m^2 and 8.7×10^{-5} s^2/m^2.

(48) French Alps (Olivry and Hoorelbeck, 1990): Badlands on black marls with swelling clay minerals in the Buëch Valley, close to the city of Serres. Poor vegetation cover. Mediterranean climate with frost action in winter and p_t around 0.9 m. Laragne basin; estimation of $h_G = 10$–15 m based upon photo. $E_{S\text{-}G(B)}$ (B = badlands) between 3.8×10^{-5} s^2/m^2 and 5.7×10^{-5} s^2/m^2.

(49) New Mexico, USA (Leopold et al., 1966): Arroyo development in the Coyote C. drainage basin vegetated by woodland with a low-density understory of grasses. Gully headcut development measurements during 3 years; erosion in clayey silty sands; $h_G = 2$–3 m; $p_t = 0.3$ m. $E_{S\text{-}G}$ between 3.1×10^{-5} s^2/m^2 and 4.7×10^{-5} s^2/m^2.

(50) Iowa, USA (Piest et al., 1975): Rolling countryside of Iowa with loess soil mantle overlying glacial till; S between 0.04 and 0.15; p_t about 0.8 m. Gullies in watersheds 1 and 2, near Treynor, monitored during the period November 1964–May 1973. Main crop: corn. $E_{S\text{-}G}$ between 6.3×10^{-6} s^2/m^2 and 7.1×10^{-6} s^2/m^2 (watershed 1) and 2.6×10^{-5} s^2/m^2 and 3.0×10^{-5} s^2/m^2 (watershed 2).

(51) Cévennes, France (Muxart et al., 1987): Valley of the Airette river, southern part of the Massif Central underlain by granites. Erosion on sandy soils and gully development on midslope sections since the Middle Ages (600–800 yrs): periods of deforestation during the foregoing centuries. Mediterranean climate: p_t between 1.5 and 1.8 m; estimation of the A_G/A ratio according to Fig. 1. $E_{S\text{-}G}$: 1.4×10^{-5} s^2/m^2 to 2.2×10^{-5} s^2/m^2.

(52) Brabant, Belgium (data Leuven, Lab. Exper. Geomorphology September 1989–May 1990): Gully headcut retreat near sunken road following the drainage line of the Ormendael basin near Leuven. Rolling landscape with loess loamy cover. Dominantly arable land and pastures; S between 0.15 and 0.20 for the steep midslope sections; p_t approximately 0.8 m. $E_{S\text{-}G}$: 1.2×10^{-5} s^2/m^2.

(53) New Mexico, USA (Malde and Scott, 1977): Contemporary arroyo cutting near Santa Fe. Stony soils and $p_t = 0.382$ m; $h_G = 2$ to 3 m: (a) "Canada de la Cueva" dissects poorly cemented loose sediments: $E_{S\text{-}G} = 2.1 \times 10^{-5}$ s^2/m^2; (b) "Pueblo Canon" entrenches alluvium indurated by caliche: $E_{S\text{-}G} = 1 \times 10^{-5}$ s^2/m^2.

(54) N. China (Tang Keli et al., 1987): Accelerated erosion in the loess plateau of northern China, in the Xingzihe River Basin. Development of 200–300 m deep canyons caused by irrational land use. Gully density 5–6 km/km^2 for an area with $p_t = 0.51$ m. According to the actual rates of erosion: $E_{S\text{-}B} = 9.1 \times 10^{-5}$ s^2/m^2. Estimation for the whole Holocene period: $E_{S\text{-}B} = 1 \times 10^{-5}$ s^2/m^2.

(55) Moldavian Tableland, Romania (Ionita, 1986): Cultivated land with steep midslope sections of the Tarina Basin. Measurement of annual gully growth rates in an area with $p_t = 0.45$–0.60 m. $E_{S\text{-}G}$ between 1.6×10^{-5} s^2/m^2 and 2.1×10^{-5} s^2/m^2.

(56) Mount St. Helens, USA (Collins and Dunne, 1986): Erosion of sand–silty tephra after destruction of forest vegetation by the 1980 eruption. Measurements at intervals on hillslopes (S around 0.45) north of Mt. St. Helens. Annual p_t around 1.4 m. Annual V_G

between 80 and 400 m^3/km^2, range derived from estimated erosion rates. $E_{S\text{-}G}$ between 2.3×10^{-6} s^2/m^2 and 2.9×10^{-5} s^2/m^2.

(57) Moldavian Tableland, Romania (Ionita, 1986): Data for the Vasilache Basin which is characterized by chernozem soils. Mainly cultivated land and soils with a high water absorption capacity. Annual precipitation: 0.45–0.60 m. $E_{S\text{-}G}$ between 3×10^{-6} s^2/m^2 and 4×10^{-6} s^2/m^2.

(58) N.S.W., Australia (Sneddon et al., 1988): Gully erosion in duplex soils in a catchment at the headwaters of Yass River, near Canberra. Erosion in improved grassland with gentle slopes: $S = 0.06$–0.07. Soils of Southern Tablelands with A-horizon on a clay-textured B-horizon. Frost–thaw action and intervention of interflow; p_t around 0.75 m. Photogrammetric monitoring program. $E_{S\text{-}G}$: 1.1×10^{-6} s^2/m^2.

(59) New Mexico, USA (Wells, 1983): Badland watersheds of the San Juan Basin (p_t around 0.2 m). Arid area with a shale-dominated lithology and with sandstones. Badland development in the Chaco River Basin: $A_G/A = 400$ $km^2/4{,}000$ km^2, postdating a period between 3,000 and 5,000 yrs. Present arid climate since mid-Holocene times. $E_{S\text{-}B}$ between 1.0×10^{-5} s^2/m^2 and 1.7×10^{-5} s^2/m^2.

(60) East Russian Plain (Boiko et al., 1991): Analysis of ravine densities, the result of gully erosion in the Volga Basin, near the city of Ulyanovsk, in undulating plains with arable land and p_t around 0.5 m. Age of the gully systems: between 100 and 150 yrs. Average width of gullies calculated according to an approach proposed by Zachar (1982, Table 74) which relates surface areas gullied to gully density. $E_{S\text{-}G}$: at the minimum 2.8×10^{-6} s^2/m^2 to 4.2×10^{-6} s^2/m^2.

Three examples illustrate the type of computations.

Imiga watershed, Burkina Faso (Mietton, 1988):

$$E_{S-G} = \frac{A_G(624\,m^2)}{A(5.3 \times 10^6\,m^2) \times P(0.56\,m) \times g(10\,m/s^2)} = 2.1 \times 10^{-5}\,s^2/m^2$$

New Mexico, Pueblo Canon (Malde and Scott, 1977):

$$E_{S-G} = \frac{V_G(1{,}770\,m^3)}{A(22.1 \times 10^6\,m^2) \times P(0.382\,m) \times g(10\,m/s^2) \times h_G(2\,m)}$$

$$= 1 \times 10^{-5}\,s^2/m^2$$

China, Xingzihe River Basin, northern loess plateau (Tang Keli et al., 1987) — $E_{S\text{-}G}$ for the whole Holocene period of 10,000 yrs:

$$E_{S-G} = \frac{A_G/A = 0.554}{P(10{,}000\,yr \times 0.5\,m/yr = 5{,}000\,m) \times g(10\,m/s^2)} = 1 \times 10^{-5} s^2/m^2$$

3.3.2. Discussion and a proposal of $E_{S\text{-}G}$ domains

Across the whole range of different climatic belts and geographical conditions, it is remarkable that $E_{S\text{-}G}$ values are so strongly concentrated within the interval 1×10^{-6}–

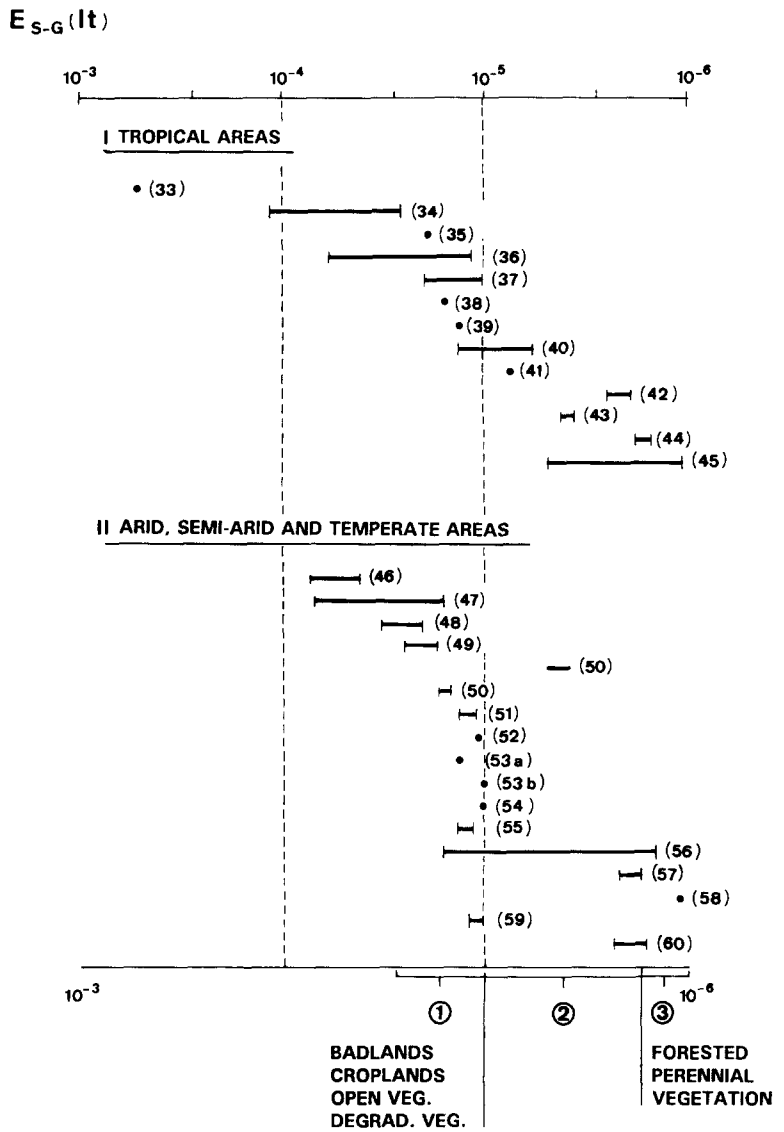

Fig. 4. $E_{S\text{-}G}$ domains for tropical and extra-tropical regions. Numbers in parentheses refer to specific sites described in the text.

1×10^{-4} s^2/m^2 with a global mean around 1×10^{-5} s^2/m^2. Two-thirds of the values fall within the range 6×10^{-6} to 3×10^{-5} s^2/m^2. $E_{S\text{-}G}$ is approximately 1×10^{-5} s^2/m^2 for strongly contrasting areas in terms of landscape and scale: Chinese loess canyons, small ravine headcuts along a sunken road in Belgium, thalweg gullying in a degraded savanna woodland in Burkino Faso, gullying under semi-arid conditions in

New Mexico, etc. How may these E_S values be explained? We have to keep in mind the basic definition and meaning of E_S which relates volumes and surface areas eroded to an expression of geomorphic energy involved. Thereby the ratio can be the same for erosional features which differ in size by several orders of magnitude and which belong to totally different geo-ecological sceneries. For example, single thalweg gullies in the degraded savanna of Burkino Faso have E_S values comparable to impressive loess badlands in northern China with entrenchments over depths of 200–300 m!

There are no indications of an overall systematic impact of the lithopedological properties of substrates on the ranking of $E_{S\text{-}G}$. This may be due to compensatory effects that govern the development of gullies which depends upon both hydraulic erosion and effects of mass wasting on sidewalls. For example, entrenchment is easier on most sandy substrates then on clayey substrates but on the other hand sidewalls of gullies in clayey materials are more prone to slumping and sliding. Higher shear strengths of the sands increase the relative stability of sidewalls cut into sandy sediments. Moreover most gully systems entrench several soil horizons or layers of different textural–structural composition and resistance. Obviously the integrated effect of such conditions can be to produce convergent V_G/h_G, A_G/A ratios as far as the type of vegetation cover is similar.

No evident correlation seems to exist between the ranking of $E_{S\text{-}G}$ values and the intensity of relief. On more than half of the sites, thalweg gullying is the dominant feature. On the volcano of Papua New Guinea, in Tanzania, Zaire, France, China and on the slopes of Mt. St. Helens gullying was embranching on full midslope sections. Yet there is no concentration of the corresponding $E_{S\text{-}G}$ values in any particular interval. On the recent Papua New Guinea volcano, massive gullying started in 1937 on bare slopes, difficult to be colonised by vegetation. Apparently the high $E_{S\text{-}G}$ value for this volcano has also to do with the presence of loose, erodible deposits.

Separation of the data between group I (tropical humid and subhumid areas) and group II (arid, semi-arid and temperate belts) does not bring about any particular ranking related to various precipitation regimes. Probably there would be some definite correlation between $E_{S\text{-}G}$ and precipitation if we had mainly to consider natural landscapes without man made changes in pedobotanical conditions. But in most of the sites referred to, ground cover by vegetation was thoroughly modified by man's activities.

Finally a dominant correlation appears between type and density of vegetation on one hand and ranking of $E_{S\text{-}G}$ values on the other hand. This results in the following sequence of $E_{S\text{-}G}$ domains proposed:

1. $E_{S\text{-}G}$ between 1×10^{-5} s^2/m^2 and 5×10^{-5} s^2/m^2
- badlands in different climate belts
- cultivated land with a predominance of cropland
- steppic areas or areas with a natural open savanna woodland
- intensively degraded grasslands and savanna areas often due to overgrazing

2. $E_{S\text{-}G}$ between 3×10^{-6} s^2/m^2 and 1×10^{-5} s^2/m^2
- partly degraded steppic woodlands or savannas with duricrusts including laterite cappings
- areas underlain by soils with a high water absorption capacity (very sandy soils, chernozems...)
- areas with mixed farming: arable land, prairies and forested slopes

3. $E_{S\text{-}G}$ between 1×10^{-6} s^2/m^2 and 3×10^{-6} s^2/m^2

– Areas with occasional gullying, predominantly thalweg gullying:
  – forested catchments with dispersed cultivation
  – perennial grasslands and savanna woodland with appreciable runoff coefficients during storm events

The predominant impact of vegetation cover can be explained:

(a) by the fact that plants and related ground cover inhibit and reduce hydraulic erosion by direct protection of topsoils;

(b) because root systems often strengthen soils and thereby increase sidewall stability.

But the situation is more complex for cropland with a seasonally changing plant cover density, with annual and perennial crops and (ephemeral) gully development, partly controlled by the complex linear infrastructure of rural areas (parcellation, lynchets, road patterns...). To this situation corresponds a high variability of $E_{S\text{-}G}$, which is demonstrated in Fig. 4 by the dispersion of values for Romania (55), Iowa (50) and the Russian Plain (60). Therefore, our proposal to link croplands with domain (1), where $E_{S\text{-}G}$ ranges between 1×10^{-5} and 5×10^{-5} s^2/m^2, must be correctly interpreted. It has to be considered as a safe estimation of maximum susceptibility for gullying in arable lands marked by a predominance of fairly erodible loams, often loess loams.

Interpolated $E_{S\text{-}G}$ values derived from the three domains can be used for prediction of A_G/A on V_G after solving formulas (32) and (30) for those parameters. Considered sites can be compared with the reference sites already quoted in order to find out the best interpolation for $E_{S\text{-}G}$. A thorough preliminary field survey, if possible, will always be of great help to an optimum achievement of such operation, especially when information on h_G is needed to calculate V_G, similar to the computation of $V_{L,DF}$ as a function of $h_{L,DF}$. In a given area both fossil and active features may give information on the possible and most likely numerical range for such parameters. The considered area A can also be compared to adjacent catchments or to similar watersheds elsewhere where gullying was or is active in order to provide information on the type of erosional system to be expected. It is desirable to underpin E_S prediction by a comparative study of catchments and by field surveys.

Take, for example, a catchment of size A delimited by a given crestline and affected by an expanding gully system which is marked by an increasing number of retreating headcuts. For a constant total runoff production the ratio A_G/A is increasing with time but most likely according to an exponential function which indicates that the rate of expansion will slow down progressively (Graf, 1977). In fact gully heads and sidewalls will be fed by decreasing runoff discharges and will therefore have their rates of recession reduced (De Ploey, 1989). An applicable $E_{S\text{-}G}$ interval can be proposed on the basis of interpolation within the above-discussed domains, or $E_{S\text{-}G}$ can be derived from direct monitoring of gully erosion during a certain period of time and subsequent computations according to relations (30) or (31). Given such $E_{S\text{-}G}$ value and p_t (the average amount of annual precipitation), a conservative estimate can be made of the age t of the whole gully system:

$$t = \frac{A_G}{E_{S-G} \cdot A \cdot p_t \cdot g} \tag{33}$$

For badlands, when A_G/A tends to a value of 1.0, the minimum age will be

$$t = \frac{1}{E_{S-G} \cdot p_t \cdot g} \tag{34}$$

with t in years, p_t (annual precipitation) in m, and $g = 10$ m/s^2.

Solving Eq. (34) means that a minimum period of time is proposed for full badland development according to a linear approach. In reality the growth rate might be rather degressive as explained higher. It is interesting to see that calculated t-values are often much higher than expected. This can be shown by the example from the Mediterranean belt. Here, it is reasonable to suppose that many badlands, which are actually situated in semi-arid to sub-humid areas (for example in SE Spain) were expanding during Quaternary times under conditions of annual rainfall amounts p_t with a maximum variance between 0.25 m and 0.75 m. To such badlands apply $E_{S\text{-}G}$ values of domain 1, between 1×10^{-5} and 5×10^{-5} s^2/m^2, which refer to gullying under semi-arid conditions or in landscapes with an open vegetation and to actual badland development in France (Olivry and Hoorelbeck, 1990), in New Mexico, USA (Leopold et al., 1966 Malde and Scott, 1977 Wells, 1983) and in N. China (Tang Keli et al., 1987). After substitution in (34), one obtains for these badlands a minimum age t_{min} between 2,700 and 40,000 yrs.

This result is strongly opposed to the hypothesis of rapid badland development in historical times, often imputed to massive forest clearance and soil degradation since Roman times. At least for SE Spain, it supports the conclusions of Wise et al. (1982) warning against an overestimation of erosion rates during the last two millenia. Our $E_{S\text{-}G}$ approach points to a full Holocene or an Upper Pleistocene age of badlands in the Mediterranean belt. It is suggested to confront this result with existing or forthcoming data issued from Quaternary research in the same areas.

It is up to the investigator, familiar with the field conditions, to define an area A, corresponding to the hydrological unit which controls gully development. In the case that pipe erosion and associated mass wasting are the dominant erosional features, expressions (30) or (32) may still be applied in calculating $E_{S\text{-}G}$. In that case it is proposed as a matter of convention to restrict V_G and A_G computations to the obviously open gullies. In some badland areas, remnants exist of the original surfaces which were entrenched by gullies. These old surfaces, sometimes dated, may serve as reference levels for defining V_G and A_G. But A_G may also be calculated for fully dissected badlands with rounded forms, studied by Schumm (1956) in the US. According to this author, mass wasting, in form of creep, contributes to the shaping of the convex crests. Similarly, in the Dinosaur Provincial Park badlands of Alberta (Canada) Bryan et al. (1978) determined experimentally that mudflows and microslumping influence the morphogenesis of steep (but not subvertical) badland slopes. This means that total sediment delivery on such gully and badland slopes results from both hydraulic erosion and mass wasting, conform with the basic concept behind $E_{S\text{-}G(B)}$, where "B" stands for badlands. Those products of erosion were evacuated through h_G, the average maximum depth of the drainage lines within A_G. Yet the definition of h_G and V_G may require a geomorphological survey of the area in order to determine the level and age of the original surface from which gullying started. It may be easier to compute the

long-term value of $E_{S\text{-}G(B)}$ by manipulating the ratio $A_{G,B}/A$, but the calculation of $P = p_t \cdot t$ in formula (32) requires at least an acceptable estimation of t, the age of the system (or, in a short-term perspective, the period of time during which the expansion of an erosional system took place and was monitored).

3.4. Rill–interrill erosion (R,IR)

3.4.1. $E_{S\text{-}R,IR}$: basic expressions and data

Rill–interrill erosion is active on slopes of areas with a more or less open natural or semi-natural vegetation but it is a particularly striking erosional system in many croplands with more or less cohesive, tilled soils. Rapid development of rill–interrill patterns often occurs on poorly protected topsoils during the period of the year when processes of sealing and crusting promote runoff generation. Sheetwash is predominant on the interrill areas whereas the first incision of rills depends upon the generation of shear stresses of concentrated flows which allow for a non-selective erosion of topsoil sediments. For silty loess loams, Govers (1985) defined such hydraulic thresholds for incipient rill formation and De Ploey (1989) developed a headcut retreat model for the regression of knickpoints and headcuts, a prominent feature of the expansion of rills and gullies. Moreover rill development is to a large extent controlled by mass movements affecting unstable headcuts and sidewalls. Therefore, similar to gullies, entrenchment and volumetric growth of rills has to be considered as the result of a process combination with interaction between hydraulic erosion and mass wasting active at a microscale. For that reason h_R, the average maximum depth of a rill system, is a parameter entering the $E_{S\text{-}R,IR}$ expression which is derived from the general Eq. (2):

$$E_{S-R,IR} = \frac{V_E}{A \cdot P \cdot g \cdot h_R} \tag{35}$$

where V_E corresponds to the total volume eroded within A by combined rill and interrill erosion. Hence,

$$V_E = V_R + V_{IR} = V_R(1 + a) \tag{36}$$

with a, the interrill erosion coefficient, corresponding to the ratio V_{IR}/V_R. Furthermore

$$V_R = m \cdot A_R \cdot h_R \tag{37}$$

where A_R corresponds to the total surface area eroded by rills whereas m is a rill shape factor ($m = 1.0$ in the case of a rectangular rill cross-section; $m = 0.5$ for a triangular cross-section). Substitution of (36) and (37) in (35) gives

$$E_{S-R,IR} = \frac{m \cdot A_R \cdot (1 + a)}{A \cdot P \cdot g} \tag{38}$$

For the Belgian loess area Govers and Poesen (1988) found V_{IR} values equal to about $0.25V_R$. For the USA, discussing the Revised Universal Soil Loss Equation (RUSLE), Renard et al. (1991) mention a values between 0.05 and 0.20. On the other hand m-values vary between 0.5 and 1.0; they may come close to 0.7–0.8 when rill

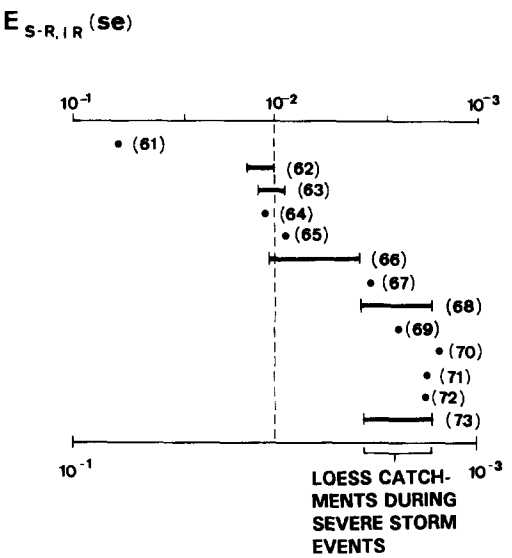

Fig. 5. $E_{S\text{-}R,IR}$ domains for single storm events. Numbers in parentheses refer to specific sites described in the text.

cross-sections present an overall trapezoidal form as is often the case. Thus, a somewhat arbitrary but reasonable simplification of relation (38) is:

$$E_{S-R,IR} = \frac{A_R}{A \cdot P \cdot g} \tag{39}$$

This formula is similar to expression (32) for gullying and again introduces the planimetric ratio A_R/A which is relatively easy to monitor. But most reported field data are on a volumetric basis. Therefore, $E_{S\text{-}R,IR}$ computations according to expression (35) require information on the average maximum depth of rills h_R, the elevation head loss parameter, linking hydraulic erosion to mass wasting.

Fig. 5 presents $E_{S\text{-}R,IR}$ values for single storm events or rill–interrill erosion which resulted from a short, well-defined rainy period. The majority of these data originate from European loess areas. Fig. 6 brings together data on an annual basis as well as some long-term information.

Geography and data of the sites belonging to the category of the single storm events can be summarized as follows, with $P = P(\text{se})$ corresponding to the total precipitation during the event(s):

(61) Southern Shaba, near the Kafubu River, Zaire (Lootens, 1983): Effect of two weeks of rainstorms, with $P(\text{se}) = 0.23$ m, on bare clayey soils developed on schists. Low sloping fields; $V_{R,IR} = 55$ m^3; $A = 6{,}000$ m^2; $h_R = 0.05$ m; $E_{S\text{-}R,IR} = 8 \times 10^{-2}$ s^2/m^2.

(62) East Anglia, UK (Evans, 1981): Gentle rolling landscape with clayey and fine loamy soils over clays. Effects of rainfall concentrated in March–April, 1969; $P(\text{se})$ estimated between 0.1 and 0.2 m; $A_R/A = 0.022$; $E_{S\text{-}R,IR}$ between 1.1×10^{-2} s^2/m^2 and 2.2×10^{-2} s^2/m^2.

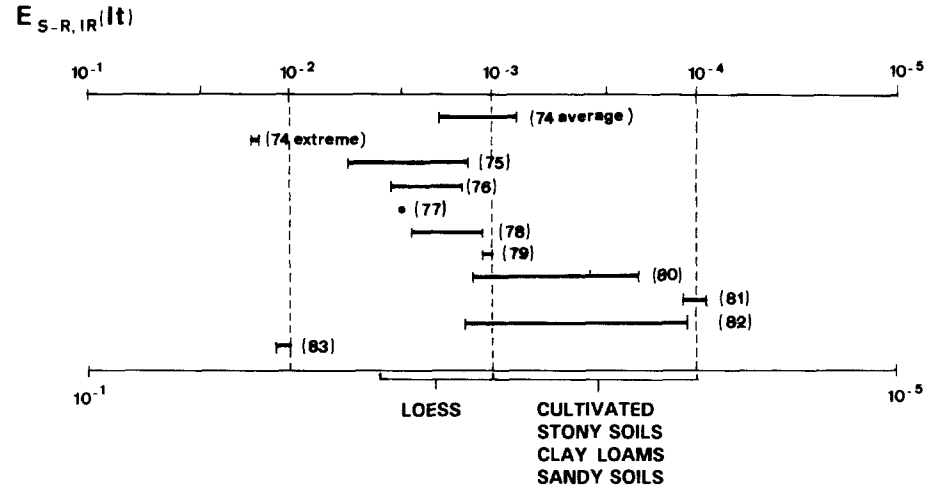

Fig. 6. $E_{S\text{-}R,IR}$ domains for annual and long-term periods. Numbers in parentheses refer to specific sites described in the text.

(63) East Sussex, UK (Boardman and Robinson, 1985): Heavy erosion on the Bevendean site after fields were sown with a grass ley and rolled. Thin rendzina soils and brown calcareous earths over chalk; S up to 0.27; P(se) about 0.25 m between 20 Sept. and 25 Oct. 1982; $V_{R,IR} = 962$ m^3; $A = 100{,}000$ m^2; $h_R = 0.2$–0.4 m; $E_{S\text{-}R,IR} = 9.6 \times 10^{-3}$ s^2/m^2 to 1.9×10^{-2} s^2/m^2.

(64) Oise, France (Peyre, 1990): Rolling gentle sloping with loamy soils and S_{max} up to 0.10; effects of heavy storm ($P = 0.052$ m) on May 10, 1986; $A_R/A = 0.0078$; $E_{S\text{-}R,IR} = 1.5 \times 10^{-2}$ s^2/m^2.

(65) Brabant, Belgium (Vandaele, 1990, pers. commun.): Effects of the 17–18 June 1986 heavy rainstorm on a cropland watershed between Leuven and Brussels; S up to 0.04; A_R defined by aerial photograph analysis = 3,600 m^2; $A = 940{,}000$ m^2; P(se) = 0.04 m; $E_{S\text{-}R,IR} = 9.6 \times 10^{-3}$ s^2/m^2.

(66) Norfolk, UK (Evans and Nortcliff, 1978): Arable land in a rolling area with S up to 0.27; typical brown earths in fine sandy loams over sand or gravel; P(se) estimated between 0.2 and 0.4 m; formation of rills and ephemeral gullies; $A_{R(G)} = 15{,}250$ m^2; $A = 610{,}000$ m^2; $E_{S\text{-}R,IR}$ between 6.3×10^{-3} s^2/m^2 and 1.2×10^{-2} s^2/m^2.

(67) Brabant, Belgium (Vandaele, 1990, pers. commun.): Cultivated land on loess in a hill-region with slope gradient S up to 0.20. Rill–interrill erosion in the Ganspoel watershed after the 17–18 June 1986 rainstorm event; $A_R = 5{,}250$ m^2 defined by aerial photograph analysis; P(se) = 0.04 m; $E_{S\text{-}R,IR} = 5.7 \times 10^{-3}$ s^2/m^2.

(68) Kent, UK (Boardman and Hazelden, 1986): Severe erosion during the autumn of 1984 in rolling cropland with loess loamy mantles on chalk (data for site 1, a 8.2 ha onion field); S up to 0.10; P estimated between 0.1 and 0.2 m; $V_{R,IR} = 101$ m^3; $A = 82{,}000$ m^2; $h_R = 0.2$ m; $E_{S\text{-}R,IR(G)}$ between 3.0×10^{-3} s^2/m^2 and 6.1×10^{-3} s^2/m^2.

(69) Flanders, Belgium (Gabriëls et al., 1977): Measurements in 1974 on a winter wheat field with a loamy sandy subsoil. Rill development on sowing lines for S up to

0.05; $P = 0.213$ m; $V_{R,IR} = 19.15$ m^3; $A = 14{,}000$ m^2; $h_R = 0.14$ m; $E_{S\text{-}R,IR} = 4.6 \times 10^{-3}$ s^2/m^2.

(70) Pomerania, Poland (Kostrzewski et al., 1989): Severe erosion on potato land during a $P(se) = 0.06$ m rainstorm in May 1983; S up to 0.26; clayey sands on sandy till; $V_{R,IR} = 50$ m^3; $A = 99{,}000$ m^2; $h_R = 0.3$ m; $E_{S\text{-}R,IR} = 2.8 \times 10^{-3}$ s^2/m^2, rather a minimum value since h_R, corresponding to the average maximum depth of rills, may be inferior to 0.3 m.

(71) Brabant, Belgium (Vandaele, 1990, pers. commun.): Aerial photograph analysis of rill patterns generated in the Kinderveld watershed during the 17–18 June 1986 rainstorm with $P(se) = 0.04$ m; S up to 0.15; mainly cropland but also forested slopes and meadows which reduce total erosion in the catchment; $A_R = 4{,}845$ m^2; $A = 3{,}800{,}000$ m^2; $E_{S\text{-}R,IR} = 3.2 \times 10^{-3}$ s^2/m^2.

(72) Sussex, UK (Boardman and Robinson, 1985): Severe erosion on Breaky Bottom site which is a meandering dry valley with stony soils and steep slopes; S up to 0.36. Effect of October 1982 rainfall totaling between 0.1 and 0.2 m; fields were sown with winter cereals in the early autumn; $V_{R,IR}$ (conservative estimation) = 101 m^3; $A = 250{,}000$ m^2; $h_R = 0.2$ m; $E_{S\text{-}R,IR} = 1.0 \times 10^{-3}$ to 2.0×10^{-3} s^2/m^2, also a conservative estimation.

(73) Brabant, Belgium (Vandaele, 1991, pers. commun.): Formula $E_{S\text{-}R,IR} = A_R/A \cdot P \cdot g$ was applied to 22 catchments, totalling about 10 km^2, which suffered from rill and interrill erosion during the period May–June 1986; $P(se) = 0.09$ m. More than 80% of the considered loess area is cropland (cereals, sugar beet, chicory, corn) and maximum slope gradients S vary between 0.10 and 0.20. Even in summer time ground cover of the fields is still limited, certainly below 50%. For each watershed the A_R/A ratio was calculated after aerial photograph analysis. All $E_{S\text{-}R,IR}$ values range within an extreme interval 1.5×10^{-3} to 9.3×10^{-3} s^2/m^2, with a definite concentration for 14/22 catchments within the interval 3.0×10^{-3}–6.0×10^{-3} s^2/m^2.

Cropland is by far predominant on all the above-considered sites. One has to expect lower $E_{S\text{-}R,IR}$ values for catchments which are partly forested or occupied by grassland or any other type of vegetation which inhibits rill development.

So-called long-term $E_{S\text{-}R,IR}$ computations apply to a minimum period of time of one year. The data presented originate from different parts of the world.

(74) Baden-Würtemberg, Germany (Eichler, 1979): Measurements of soil erosion in a hilly loess-covered area of Kraichgau with S up to 0.10; annual p_t: 0.75–0.80 m; evaluation of the average denudation rates since medieval times: 0.35–0.50 mm/yr but up to 10 mm/yr during extreme years. Average $E_{S\text{-}R,IR}$: between 9.0×10^{-4} s^2/m^2 and 3.3×10^{-3} s^2/m^2. For extreme years: between 2.5×10^{-2} s^2/m^2 and 2.7×10^{-2} s^2/m^2.

(75) Hesbaye, Belgium (Bollinne, 1978): Calculations of denudation rates for the last 145–170 yrs in the loess-covered hill-region of Hesbaye. Volumetry derived from dated colluvial deposits in closed depressions surrounded by midslopes with maximum S up to 0.10; $V_{R,IR}$ between 8.5 and 10.4 m^3/ha; $p_t = 0.7$–0.8 m; h_R between 0.02 and 0.05 m. $E_{S\text{-}R,IR}$ between 2.1×10^{-3} s^2/m^2 and 7.4×10^{-3} s^2/m^2.

(76) Brabant, Belgium (Desmet, 1986): Estimation of the denudation rate for the last 1,000 yrs in the loess belt near Leuven (Ganspoel catchment). Calculations based on the

average depth over which Holocene brown earths were truncated by erosion since this loess area, with average maximum slope gradients $S = 0.10–0.15$, became mainly cropland; $h_R = 0.03–0.05$ m; $p_t = 0.8$ m; $V_E = 1.33$ m^3 for $A = 1$ m^2; $E_{S\text{-}R,IR} = 3.3 \times 10^{-3}–5.5 \times 10^{-3}$ s^2/m^2.

(77) Brabant, Belgium (Govers, 1985): Observations and measurements in 62 fields near Leuven, with rill/interrill erosion during the autumn–winter periods 1982, 1983, 1984 and 1985 when overall crop cover protection was very low. Silty to sandy loamy topsoils prone to sealing and crusting. Average rill depth h_R varied between 0.03 and 0.05 m in catchments with maximum slope gradients S between 0.08 and 0.15. Average P for that period of the year (October–March): 0.45 m. Application of expression (39): $E_{S\text{-}R,IR} = A_R/(A \cdot P \cdot g) = 5.1 \times 10^{-3}$ s^2/m^2, the average value for all 62 fields.

(78) Somerset, UK (Colborne and Staines, 1985): Follow-up of erosion on 19 winter cereals fields, on very fine sandy and silty soils with poor topsoil structure. Study period: October 1982–June 1983; $P = 0.6–0.8$ m; S between 0.06 and 0.10; development of many shallow rills often less than 2 cm deep; $E_{S\text{-}R,IR} = 5.4$ m^3/(10,000 m^2 × (0.6 × 0.8 m) × 10 m/s^2 × (0.02–0.05 m)) = 1.4×10^{-3} s^2/m^2 to 4.5×10^{-3} s^2/m^2.

(79) Paris Basin, France (Auzet et al., 1993): Measurements on rill erosion in 20 catchments with croplands belonging to the rolling landscape of the Paris Basin, with sandy and loamy soils on chalk or on Tertiary deposits; S_{max} inferior to 0.10; observation period: October 1988–April 1989; P around 0.5 m; without severe rainstorm events; rills on slopes and often flat thalweg rills in valley bottoms; calculation of an average $E_{S\text{-}R,IR}$ for mean h_R supposed to vary between 0.03 m and 0.04 m: $E_{S\text{-}R,IR} = 2.0$ m^3/(10,000 m^2 × 0.5 m × 10 m/s^2 × (0.03–0.04 m)) = 1.0×10^{-3} s^2/m^2 to 1.3×10^{-3} s^2/m^2.

(80) Yorkshire, UK (Ellis, 1991): Calculations of past and present chalkland soil erosion in the Yorkshire Wolds. Maximum erosion rates of 0.3–0.4 kg/m^2 · yr over the past two or three centuries calculated for arable land on $S = 0.09–0.17$ slopes by comparing thinning in cultivated soils with that in soils beneath woodland planted during the Enclosure movement; p_t estimated between 0.6 and 0.7 m; for h_R we propose an extreme possible range between 0.03 and 0.10 m; $E_{S\text{-}R,IR} = (2.5–3.3$ m$^3)$/[10,000 m^2 × (0.6–0.7 m) × 10 m/s^2 × (0.03–0.10 m)] = 3.6×10^{-4} s^2/m^2 to 1.8×10^{-3} s^2/m^2.

(81) Pyrenees, Spain (Ruiz-Flano, 1991, pers. commun.): Rill/interrill erosion since about 70 yrs on abandoned cultivated land actually marked by a matorral vegetation. Measurements on the experimental area of Aisa, Huesca with stony soils on marls and sandstones; maximum S up to 0.30; annual p_t around 0.9 m; $E_{S\text{-}R,IR} = (A_R/A = 0.06–0.10)$/[(70 yr × 0.9 m/yr = 63 m) × 10 m/s^2] = 9.6×10^{-5} s^2/m^2 to 1.6×10^{-4} s^2/m^2 (maximum depth of rills = 0.5 m).

(82) Champagne Humide, France (Laurain and Marre, 1991): Calculations of low erosion rates for the last 500 yrs in a rolling landscape with forests, meadows and cultivated land on sandy and clayey soils; S between 0.03 and 0.04 m; h_R around 0.01 m; annual $p_t = 0.7$ m; computations based on the amounts of eroded material trapped in small ponds. $E_{S\text{-}R,IR}$ within the range $1.4 \times 10^{-4}–2.1 \times 10^{-3}$ s^2/m^2.

(83) Kathiorin Basin, Kenya (Sutherland and Bryan, 1991): Measurements in semi-arid

Kenya in small catchments (Blue Subbasin and North Subbasin) covered by an open Acacia thorn-scrubland underlain mainly by poorly-sorted silty clays with minor sands and granules, with a coarse lag deposit of pebbles and boulders; $P = 0.64$ m; some steep slopes (S_{max} between 0.18 and 0.45) with rill depths h_R between 0.045 and 0.065 m. $E_{S\text{-}R,IR} = 1.1 \times 10^{-2}$ s^2/m^2 to 1.7×10^{-2} s^2/m^2. Calculation for the Blue Basin: $E_{S\text{-}R,IR} = (V_E = 83 \text{ m}^3)/[(A = 11{,}600 \text{ m}^2) \times (P = 0.64 \text{ m}) \times (g = 10 \text{ m/s}^2) \times (h_R = 0.065 \text{ m})] = 1.7 \times 10^{-2}$ s^2/m^2.

3.4.2. *Comments and $E_{S\text{-}R,IR}$ domains*

According to the $E_{S\text{-}R,IR}$ model, rill–interrill erosion appears to be a more efficient process combination than long-term mass wasting or gullying for which E_S-values range between 1×10^{-6} s^2/m^2 and 1×10^{-4} s^2/m^2 whereas for rill/interrill erosion the interval 1×10^{-4}–1×10^{-2} s^2/m^2 covers all available data. This means that for the same amount of precipitation P, the ratio V_E/h is on the average two orders of magnitude larger for rill/interrill erosion than for the other mentioned process combinations and by definition this is also true for the planimetric ratio A_R/A. In a geomorphological sense rill/interrill erosion is an efficient process combination causing overall planation and reduction of relative relief up to gentle sloping crest belts. This is certainly true for croplands where tillage operations and the whole agricultural system promote rill/interrill erosion. Such planation supposes an important lateral component of erosion which in the case of the rill/interrill system results from sheetwash on the interrill areas, from the multiplication of rills and from the widening and receding of expanding rills. Such a system is an expression of relative high erosional susceptibility of catchments. It contrasts with watersheds exclusively eroded by a limited number of deep gullies, eventually one major thalweg gully. Here, vertical erosion prevails and relative relief increases proportionally to the term h_G which expresses the loss of potential energy.

In such catchments erosional susceptibility is generally lower although erosion forms are more striking than in the case of rill/interrill erosion. This comes out from comparing $E_{S\text{-}G}$ values (Fig. 4) with the $E_{S\text{-}R,IR}$ data (Figs. 5 and 6). In reality the E_S model opposes lateral to vertical erosion through the consideration of the terms $V_E/(A \cdot h)$ and A_E/A and it estimates erosional susceptibility directly proportional to the latter term. Such approach makes sense not only in a geomorphological perspective but also in relation to erosion control. In fact, agressive rill/interrill erosion will affect relatively large surface areas in watersheds to be protected by adequate techniques. In case of exclusive gullying, causing the same volumetric effect V_E, erosion control works can be limited to a restricted area A_G because most slope sections were resistant to scouring and rill initiation. After all, the sole (thalweg) gullying a in catchment with low erosional susceptibility is no more than the morphological expression of erosion limited to the major drainage line(s) where hydraulic forces reach their maximum and detachment capacity is at its maximum because overland flow often is unable to scour most slope sections. Under such conditions erosional susceptibility $E_{S\text{-}G}$, for the same amount of rainfall P, will generally be inferior to most $E_{S\text{-}R,IR}$ values recorded. Even in badlands, where A_G/A comes close to unity, $E_{S\text{-}G(B)}$ remains within the range 1×10^{-6}–1×10^{-4} s^2/m^2 because badlands are of considerable age, of the order of millenia, as already explained higher.

Fig. 5 indicates that at least for cropland of the European Plain, with loamy soils on a rolling topography, $E_{S\text{-}R,IR}$ varies between 1×10^{-3} s^2/m^2 and 1×10^{-2} s^2/m^2. Within this interval, the ranking of the obtained values cannot be correlated neither with any systematic topographic factor nor with total amount of rainfall P. As information on other rainfall characteristics is lacking no speculations can be formulated in that direction; relatively high rainfall intensities may be an explanation for the highest $E_{S\text{-}R,IR}$ value in Shaba but this is pure hypothesis. On the other hand some arguments can be forwarded to explain the ranking of the other sites starting with the lowest $E_{S\text{-}R,IR}$ (se, single events) values:

(1) On the Sussex site (72), the erosion rates might have been considerably reduced by the presence of stony topsoils;
(2) In the Kinderveld watershed (71), about 20% of the total area is composed of forested slopes and pastures with a supposed lower erodibility than arable land;
(3) The Pomeranian site (70) and the site in Flanders (69) have sandy subsoils in common, in contrast with the loamy soils of the other sites. The lower erosion rates can be explained by relatively lower runoff coefficients and a slightly lower erodibility of sandy material compared with silty loams. Recently, Römkens et al. (1987) showed the soil erodibility factor K of the USLE for sandy material to be less than the high values found for silty material.

For (loess) loamy cropland, $E_{S\text{-}R,IR}$(se) varies between 1×10^{-3} s^2/m^2 and 1×10^{-2} s^2/m^2. It looks preferable to consider the interval 3.0×10^{-3} s^2/m^2 to 6.0×10^{-3} s^2/m^2 as a safe, conservative estimation of the erosional susceptibility of loess catchments during severe rainstorm events. The minimum threefold increase or decrease of $E_{S\text{-}R,IR}$(se) for these areas may not surprise:

(1) Recent experiments (Govers et al., 1990, Govers, 1991) show that the erosion resistance of a loamy material is extremely sensitive to variations in initial moisture content. Initially dry soils are at least three times more erodible than wet soils;
(2) According to these authors compaction seems to be effective in reducing soil loss only when the soil is sufficiently wet;
(3) The impact of crop cover density on reducing soil loss may not be overestimated, especially not the influence of canopy cover because leaf storage capacity for water is limited and stemflow production during severe storms stimulates erosion. Towards the summer, crop cover, especially direct ground cover, has a protective effect. But during a large part of the year most of the fields in the loess belt are close to the state of bare surfaces on which runoff production reaches a maximum after topsoils became nearly completely sealed and crusted;
(4) Of course one has to take into account rainfall erosivity which in Europe tends at a maximum during the warmer periods of the year. A global appreciation of all these factors and their impact may guide users of the E_S model when selecting an appropriate interval for $E_{S\text{-}R,IR}$(se) within the proposed range 1×10^{-3}–1×10^{-2} s^2/m^2.

Calculation of $V_{R,IR}$ according to expression (35) supposes information on the average maximum depth h_R of rills and ephemeral gullies. Several hundreds of data on h_R were collected by the Leuven laboratory in the Brabant loess area during the last two decades. Moreover, some information could be gained from the above-mentioned

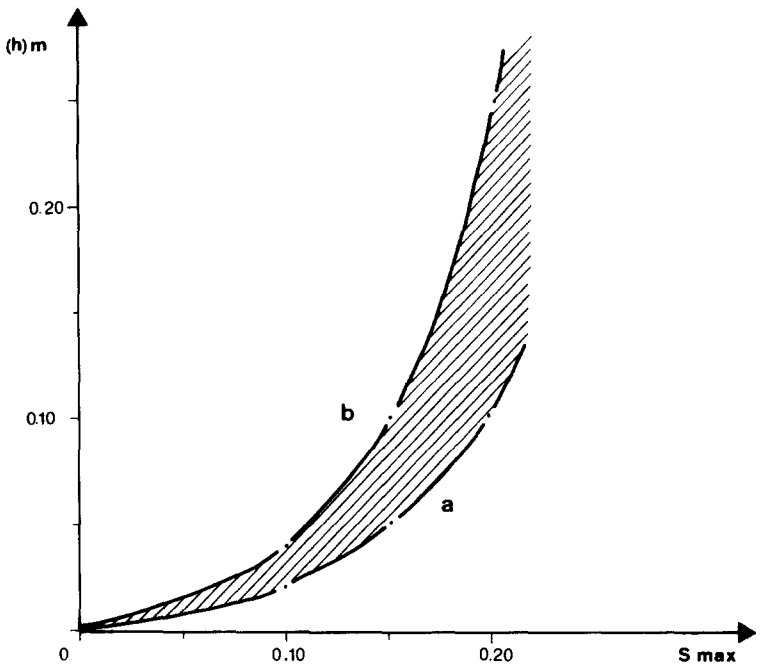

Fig. 7. Non-linear relationship between h_R and S_{max}.

literature which provided data for the $E_{S\text{-}R,IR}$ calculations. All these examples refer to croplands on loamy soils in areas where relative relief is that of gentle rolling plains up to hill regions with average maximum slope gradients S_{max}, for midslope sections, between 0.10 and 0.20. Fig. 7 shows the non-linear relationship between h_R and S_{max}. The h_R intervals result from erosion during one full growth season, a period of about 9 months between tillage and harvest. They also apply to the effects of extreme events during which rill development, in terms of A_R/A, is comparable to patterns resulting from one "normal" year. The variance of h_R increases in areas with more pronounced relief; manifestly this expresses the differential impact on rill and ephemeral entrenchment of a large number of field conditions related to rainfall characteristics, topography, flow patterns partly related to the impact of linear infrastructural elements in cultivated land (roads, parcellation...), the multilayered aspect of soils etc. It is suggested to take into consideration the full possible variance of h_R when estimating $V_{R,IR}$ for catchments of the loess belt marked by a given average S_{max}. A subsequent thorough field survey may help to delineate eventually a narrower h_R interval. Thereby, at least in the European loess areas, one discriminative criterion merits attention: clay content of the arable layer like remnants of a pronounced B_t-horizon or compact plough pans. The overall impact of those factors is to reduce h_R, the average maximum depth of rills and ephemeral gullies, especially during wet seasons or wet years when topsoil moisture contents remain high (current field observations made by members of the Leuven laboratory).

$E_{S\text{-}R,IR}$(lt) (long-term erosional susceptibility coefficient) values for loess areas defi-

nitely shift to an interval 1×10^{-3}–6×10^{-3} s^2/m^2 (Fig. 6). For a wet year with low-intensity rainfall, 1×10^{-3} s^2/m^2 is an indicative value, whereas 2×10^{-3}–3×10^{-3} s^2/m^2 certainly is a rather conservative estimation for average long-term field conditions in loess croplands. Values down to 1×10^{-4} s^2/m^2 are representative for cultivated land with stony soils, clay loams or sandy soils [the Yorkshire site (80), the Champagne site (81), the site in Spain (82)]. In the case of the Champagne site, a reduction of rill/interrill erosion on forested slopes and in pastures appears. Here, comparing to full cropland, there are good reasons to multiply $E_{S\text{-}R,IR}$ (full cropland) with a reduction coefficient CR:

$$CR = 1 - \frac{A_{F,P}}{A} \tag{40}$$

with $A_{F,P}$ corresponding to the total surface area under forests and/or pastures. In that case, solving (39) for A_R gives:

$$A_R = CR \cdot E_{S-R,IR} \cdot A \cdot P \cdot g = (A - A_{F,P}) \cdot E_{S-R,IR} \cdot P \cdot g \tag{41}$$

and solving (35) for $V_{R,IR}$ gives:

$$V_{R,IR} = (A - A_{F,P}) \cdot E_{S-R,IR} \cdot P \cdot g \cdot h_R \tag{42}$$

In the Kinderveld catchment (73) (Brabant, Belgium), $E_{S\text{-}R,IR}$ for the June 1986 rainstorm was equal to 3.2×10^{-3} s^2/m^2 when the whole watershed, including 20% $A_{F,P}$, was considered. Thus, according to (40), CR = 0.8, and for the sole cropland, $E_{S\text{-}R,IR} = (3.2 \times 10^{-3}\ s^2/m^2)/0.8 = 4.0 \times 10^{-3}\ s^2/m^2$.

The Katiorin basin (83), with the highest (1.1×10^{-2}–1.7×10^{-2} s^2/m^2) $E_{S\text{-}R,IR}$ values, falls within the semi-arid belt of Kenya and is partly underlain by silty clays belonging to vertisol types. Therefore, its high erosional susceptibility is not surprising: under such conditions swelling and dispersion of clays, combined with dessication effects, can lead to high rates of erosion as was demonstrated by intensive research in the valley of the Red Deer River, Alberta, Canada (Campbell, 1970, Bryan et al. 1978) and in the badlands of southeastern Spain (Imeson and Verstraten, 1986, Gerits et al., 1987). Looking for the differential erodibility of clayey topsoils, unpublished data bring Poesen (pers. commun.) to the conclusion that often these clayey topsoils behave as resistant material in humid areas whereas they are very sensitive to rill/interrill erosion in semi-arid belts.

Similar to the approach proposed in Section 2.7 for expressions (9) to (15), one may compare single storm effects (se) with long-term rill/interrill erosion (lt). The condition $A_R(se) = A_R(lt)$ will be met if $t = P(se)/B \cdot p_t$ (expression 13).

A numerical example related to the Brabant loess area may illustrate the meaning of this relationship. During the 17–18 June 1986 rainstorm in the Kinderveld watershed, $P(se)$ amounted to 0.04 m and $E_{S\text{-}R,IR}(se)$ was equal to 3.4×10^{-3} s^2/m^2, for cropland. In this part of Central Belgium annual precipitation $p_t = 0.8$ m and in accordance with the delineation of major $E_{S\text{-}R,IR}$ domains for loess belts, 2.0×10^{-3} to 3.0×10^{-3} s^2/m^2 is a safe estimation of the long-term erosional susceptibility. Solving relation (13), with $B = E_S(lt)/E_S(se)$, gives $t = 0.07$ to 0.10 yr, i.e. between 26 and 37 days, or approximately 1 month. This means that, in terms of rilled surface areas A_R, one month

of erosion under long-term conditions should have the same effect as the 17–18 June 1986 storm event. According to expression (15) above:

$$t = T(\text{se}) = P(\text{se})/B \cdot p_1$$

which expresses, in years, the minimum recurrence interval of the $P(\text{se}) = 0.04$ m single extreme event. In reality $T(\text{se})$ is far superior to 0.07–0.10 yr because one has to consider the local rainfall regime, especially the magnitude–frequency of daily rainfall. In that respect an interesting approach to the identification of morphoclimates was discussed by Ahnert (1987) who states that the commonly observed distribution of daily rainfall amounts, p_{24} (equal to $P(\text{se})$ in our case), as a function of $\log_{10}T$ (T is the recurrence interval in yrs) is approximately linear and described by:

$$p_{24} = p_1 + K \cdot \log_{10}T \tag{43}$$

so that

$$T = 10^{[(p_{24}-p_1)/K]} \tag{44}$$

where K corresponds to the coefficient of the semilogarithmic regression which is specific for a given station: p_1 is the daily rainfall amount with the recurrence interval $T = 1$ year; $p_1 + K$ is the daily amount with $T = 10$ yrs. K can be used as a "decadic" two-number magnitude–frequency index $\text{MFI} = p_1/K$.

For the station of Tienen, which belongs to the same climatic zone as the above-mentioned Kinderveld watershed, $p_{24} = 29 + 27.3\log_{10}T$ (p_{24} in mm), and for $p_{24} = 0.04$ m $= P(\text{se})$, $T = 2.5$ yrs, which is far superior to the above-calculated period t, which is equal to 0.07–0.10 yr. For the $E_{\text{S-R,IR}}$ analysis of single storm events, expression (43) may replace the term P in the basic formulae (35) and (39).

It must be stressed that the h_R–S_{max} diagram (Fig. 7) applies mainly to very erodible loess loam profiles. One expects the lowermost delineating curve (a) to represent maximum h_R values either for definite clayey soils or for sandy substrates, the former ones being more resistant to incision and the latter ones more prone to sheet erosion induced by topsoil liquefaction. Also, the diagram may not be representative for steep cultivated mountain slopes, with average slope gradients above 0.20, where other factors counteract excessive rill entrenchment:

(1) stony topsoil material which reduces overall erodibility and promotes forms of sheet erosion;
(2) the predominance, on mountain slopes, of fine soil material with a specific erodibility inferior to loess loams;
(3) the commonly observed tendency on steep slopes (for example in badlands) towards an increase of the specific density of rill networks, corresponding to a relative increase of the A_R/A ratio, with close spacings of many small rills each of them marked by limited depths. In other words cultivated steep mountain slopes, although characterized by higher erosion rates, tend more towards the development of sheet erosion systems or rill/interrill systems with a strong sheet erosion component on the interrills. A recent extensive survey by Moeyersons (1989) of erosional systems in Rwanda is in line with these conclusions.

4. Some general remarks

This article refers only to basic expression (3), which is related to all processes of mass wasting and water erosion, except pure sheet wash. There is no doubt that the E_S-model is a flexible tool, easily used by the introduction of only a few, mostly easily available, parameters. Moreover, it appears that any process covered by (3) results in characteristic E_S-values within a given pedo-botanical context. Also, for mass movements (Figs. 1 and 2), there exists a net distinction between single event (se) and long-term (lt) erosional susceptibility. This distinction also exists for rill/interrill combinations (Figs. 5 and 6). Data on gullying (Fig. 4) and creep (Fig. 3) cover periods of at least one year, and, therefore, have to be considered as long-term events. But it is obvious that single events of creep and gullying should give rise to higher values than their long-term counterparts, just as in the case of landslides/debris flows and rill/interrill erosion.

This characteristic ranking tells something about the efficiency of the erosional processes involved. However, it also forms a very powerful tool (once it has been accurately established in reference sites) for checking an adjacent catchment on other parameters one is interested in. The example of the age calculation of badlands in Spain is a good example of this. But, depending on the data that are available, it is evident that also p_t, the annual rainfall, or h, the mean depth of incision of the erosional forms, can be calculated.

Also, it is clear that the E_S-model offers an opportunity to calculate predictions. For example, the effects introduced by a shifting of climatic belts can be predicted with the help of E_S-values gathered in areas where the expected climate actually exists.

A lot of work remains to be done however. For example, there is the need for a closer definition of the E_S ranking for the processes discussed in this article. Also, E_S calculations and ranking for the processes not treated in this text (sheet erosion, wind erosion, etc.) are necessary. It will be a real challenge to elaborate the basic expressions (4) and (5), where kinetic instead of potential energy is involved in the denominator.

(J.M. & D.G.)

5. List of symbols and variables

a interrill erosion coefficient ($a = V_{IR}/V_R$)
A size of the area (hydrological unit) for which the E_S-coefficient is calculated
A_E size of area effectively eroded
$A_{F,P}$ size of area covered by forests and/or pastures $B = E_S(lt)/E_S(se)$
CR reduction coefficient [$CR = 1 - (A_{F,P}/A)$]
D distance, along the soil surface, of upstream retreat of a headcut
E_r erodibility coefficient
E_S coefficient of erosional susceptibility
g acceleration due to gravity
h elevation head loss, corresponding to the mean depth over which a soil volume V_E was removed
h_a average depth of denudation
h_{cr} critical height of collapsing sidewalls
h_w depth of weathering mantle
K regression coefficient in the Ahnert (1987) equation

lt long-term event(s)
L total slope length
m rill shape factor
p_1 daily rainfall amount with a recurrence interval of 1 year
p_{24} daily rainfall amount
p_t total precipitation/m^2, per unit of time t
P total volume of water precipitated per m^2
Q total discharge of the flow causing plunge-pool erosion
ρ_s mean bulk density
R hydraulic radius
se single storm event(s)
S gradient of slope
S_{max} maximum gradient of slope
t time
T recurrence interval
u mean velocity
u_0 flow shear velocity
V volume
V_E total soil volume, eroded within a surface area A
V_P total volume of water, precipitated in the catchment A during a time t
V_T total eroded volume (of sediment)
w width of a headcut
W total width of the cross-section(s) through which creeping material is evacuated
W_r average weathering rate

Subscripts
B badlands or badland erosion
C creep or creep erosion
CF congelifluction or congelifluction erosion
DF debris flow(s) or debris flow erosion
G gullies or gully erosion
IR interrill or interrill erosion
L landslide(s) or landslide erosion
R rill(s) or rill erosion

Acknowledgements

J.M. and D.G. are grateful to F. Ahnert, M. Kirkby and J. Poesen who made several constructive editorial comments during the preparation of the manuscript.

References

Ahnert, F., 1987. Approaches to dynamic equilibrium in theoretical simulations of slope development. Earth Surf. Process. Landforms, 12: 3–15.

Auzet, A.V., Boiffin, J., Papy, F., Ludwig, B. and Maucorps, J., 1993. Rill erosion as a function of the characteristics of cultivated catchments in the North of France. Catena, 20: 41–62.

Basu, S.R. and Ghatowar, L., 1988. Landslides and soil erosion in the Gish drainage basin of the Darjeeling Himalaya and their bearing on North Bengal floods. Etud. Geomorph. Carpatho–Balcanica, 22: 105–122.

Bentley, S.P. and Smalley, I.J., 1984. Landslips in sensitive clays. In: D. Brunsden and D.B. Prior (Editors), Slope Instability. Wiley, London, pp. 457–490.

Boardman, J. and Hazelden, J., 1986. Examples of erosion on brickearth soils in East Kent. Soil Use Manage., 2: 105–108.

Boardman, J. and Robinson, D.A., 1985. Soil erosion, climatic vagary and agricultural change on the Downs around Lewes and Brighton, autumn 1982. Appl. Geogr., 5: 243–258.

Boiko, F., Butakov, G., Dvinskikh, A., Dedkov, A., Korotina, N., Lapteva, H., Mozzherin, V., Rysin, I., Nazarov, N. and Tukayev, R., 1991. Territorial analysis of ravine density in the east of the Russian Plain. In: Geomorphological Processes and Environment, Abstracts of Papers, Kaza-Comtag Symposium, pp. 16–18.

Bollinne, A., 1978. Study of the importance of splash and wash on cultivated loamy soils of Hesbaye (Belgium). Earth Surf. Process., 3: 71–84.

Bonnard, C., 1983. Determination of slow landslide activity by multidisciplinary measurement techniques. In: Int. Symp. Field Measurements in Geotechnics, Zurich, pp. 619–638.

Bryan, R.B., Yair, A. and Hodges, W.K., 1978. Factors controlling the initiation of runoff and piping in Dinosaur Provincial Park badlands, Alberta, Canada. Z. Geomorphol., Suppl., 29: 151–168.

Campbell, I., 1970. Erosion rates in the Steveville Badlands, Alberta. Can. Geogr., 14: 202–216.

Cancelli, A., Pellegrini, M. and Tonnetti, G., 1984. Geological features of landslides along the Adriatic coast (Central Italy). In: Proc. 4th Int. Symp. on Landslides, Toronto, Vol. 2, pp. 7–12.

Chasovnikova, E.A., 1990. Stationary observations in the Volga–Sviaga interfluve. In: A.P. Dedkov (Editor), IGU-COMTAG Guide on geomorphology: Middle Volga. Kazan University Press, Kazan, pp. 79–80.

Ciesiolka, C., 1987. Catchment management in the Nogoa watershed. Austr. Water Res. Council, Project 80-128, 204 pp.

Coelho Netto, A.L., Fernandes, N.F. and De Deus, C.E., 1988. Gullying in the south-eastern Brazilian Plateau, Bananal (SP). IAHS Publ., 174: 35–42.

Colborne, G.J.M. and Staines, S.J., 1985. Soil erosion in South Sommerset. J. Agric. Sci., 104: 107–112.

Collins, B.D. and and Dunne, Th., 1986. Erosion of tephra from the 1980 eruption of St Helens. Bull. Geol. Soc. Am., 97: 896–905.

Cruz, O., 1974. A Serra do Mar e o Litoral na area de Caraguatatuba. Inst. Geogr. Univ. Sao Paulo, Serie Teses e Monogr., 11.

De Ploey, J., 1989. Erosional systems and perspectives for erosion control in European loess areas. Soil Technol. Ser., 1: 93–102.

De Ploey, J., 1990. Modelling the erosional susceptibility of catchments in terms of energy. Catena, 17: 175–183.

De Ploey, J., 1991a. L'Erosion de bassins versants: analyses et prévisions selon le modèle E_S. Physico-Géographie, 22–23: 7–12.

De Ploey, J., 1991b. Bassins versants ravinés: analyse et prévisions selon le modèle E_S. Bull. Soc. Géogr. Liège, 27: 69–76.

Desmet, P., 1986. Bijdrage tot de kwantificering van de totale akkererosie op lemige gronden. M.Sc. Thesis, Katholieke Universiteit Leuven, 294 pp.

Dietrich, W.E. and Dunne, T.H., 1978. Sediment budget for a small catchment in mountainous terrain. Z. Geomorphol., Suppl., 29: 191–206.

Dymond, J.R. and Hicks, D.L., 1986. Steepland erosion measured from historical aerial photographs. J. Soil Water Conserv., 41: 252–255.

Eichler, H., 1979. Bodenerosion in Maïs- und Rübenkulturen des Kraichgaues. In: Seminar Soil Erosion In Temp. Non Mediterranean Climate, Strasbourg–Colmar, pp. 145–151.

Ellen, S.D. and Wieczorek, G.F., 1988. Landslides, floods and marine effects of the storm of January 3–5 1982 in the San Francisco bay region. U.S. Geol. Surv., Prof. Paper 1434, 314 pp.

Ellis, S., 1991. Past and present chalkland soil erosion: examples from the Yorkshire Wolds. In: Abstr. Conf. Hist. and Archeol., London, p. 16.

Evans, R., 1981. Assessments of soil erosion and peat wastage for parts of East Anglia, England. In: R.P.C. Morgan (Editor), Soil Conservation. Wiley, London, pp. 521–532.

Evans, R. and Nortcliff, S., 1978. Soil erosion in North Norfolk. J. Agric. Sci., 90: 185–192.

Finlayson, B., 1981. Field measurements of soil creep. Earth Surf. Process. Landforms, 6: 35–48.

Gabriëls, D., Maene, L., Lenvain, J. and De Boodt, M., 1977. Possibilities of using soil conditioners for soil erosion control. In: D.J. Greenland and R. Lal (Editors), Soil Conservation and Management in the Humid Tropics. Proc. Int. Conf. on Soil and Management in the Humid Tropics, Abadan, 1975, pp. 99–108.

Gerits, J., Imeson, A.C., Verstraten, J.M. and Bryan, R.B., 1987. Rill development and badland regolith properties. In: R.B. Bryan (Editor), Rill Erosion. Catena Suppl., 8: 141–160.

Govers, G., 1985. Selectivity and transport capacity of thin flows in relation to rill erosion. Catena, 12: 35–49.

Govers, G., 1991. Rill erosion on arable land in central Belgium: rates, controls and predictability. Catena, 18: 133–155.

Govers, G. and Poesen, J., 1988. Assessment of the interrill and rill contributions to total soil loss from an upland field plot. Geomorphology, 1: 343–354.

Govers, G., Everaert, W., Poesen, J., Rauws, G., De Ploey, J. and Lautridou, J.P., 1990. A long flume study of the dynamic factors affecting the resistance of a loamy soil to concentrated flow erosion. Earth Surf. Process. Landforms, 15: 313–328.

Graf, W.L., 1977. The rate law in fluvial geomorphology. Am. J. Sci., 277: 178–191.

Haeberli, W., Gamper, M., Zimmerman, M. and Kienholz, H., 1989. Field trip D 4. In: Second Int. Conf. on Geomorph., Frankfurt. Geoöko-Forum, 1: 265–298.

Hiura, H. and Murakimi, K., 1981. Studies of sediment production on mountain slopes. IASH Publ., 133: 257–266.

Hupp, C.R., 1987. Dendrogeomorphic evidence and dating of recent debris flows on Mount Shasta, Northern California. U.S. Geol. Surv., Prof. Paper 1396-B, 33 pp.

Imeson, A.C. and Verstraten, J.M., 1986. Erosion and sediment generation in semi-arid and mediterranean environments: the response of soils to wetting by rainfall. J. Water Res., 5: 388–418.

Ionita, I., 1986. Results of soil erosion study and conservation treatments in the Birlad Tablelands. Z. Geomorphol. Suppl., 58: 107–119.

Jahn, A., 1981. Some regularities of soil movement on the slope as exemplified by the observations in Sudety Mts. Trans. Jap. Geomorphol. Union, 2: 321–328.

Jahn, A. and Cielinska, M., 1974. The rate of soil movement in the Sudety Mountains. Abh. Ak. Wiss. Göttingen, Math. Phys. Kl., 29: 86–100.

Jones, F.O., 1973. Landslides of Rio de Janeiro and the Serra das Araras escarpment, Brazil. U.S. Geol. Surv., Prof. Paper 697, pp. 1–42.

Kelsey, H.M., 1980. A sediment budget and an analysis of geomorphic process in the Van Duzen River Basin, north coastal California, 1941–1975. Bull. Geol. Soc. Am., 91: 190–195.

Kienholz, H., Lehman, C., Goggisberg, C., Loat, R. and Hegg, C., 1991. Bedload budget in Swiss mountain torrents with respect to the disasters in 1987. Z. Geomorphol. Suppl., 83: 53–62.

Kostrzewski, A., Klimczak, P., Stach, A. and Zwolinski, Z., 1989. Morphological effects of heavy rainfall (24 May, 1983) over relief features of the scarpland in the middle Parseta valley, West Pommerania, Poland. Quaest. Geogr., 2: 101–110.

Laurain, M. and Marre, A., 1991. Un essai d'évaluation de la vitesse de l'érosion depuis le Moyen-Age: l'example de la Champagne humide (France). Physico-Géographie, 22–23: 123–129.

Leopold, L.B., Emmett, W.W. and Myrick, R.M., 1966. Channel and hillslope processes in a semi-arid area New Mexico. Geol. Surv. Prof. Paper 352-G: 193–253.

Lootens, M., 1983. Erosion agricole accélérée sur sol nu au Shaba méridional (Zaïre). Ann. Fac. Sci., Lubumbashi, 3: 1–6.

Lundgren, L. and Rapp, A., 1974. A complex landslide with destructive effects on the water supply of Morogoro Town, Tanzania. Geogr. Ann., 56A: 3–4.

Malde, H.E. and Scott, A.G., 1977. Observations of contemporary cutting near Santa Fe, New Mexico, U.S.A. Earth Surf. Process., 2: 39–54.

Masamu, A., 1985. Contemporary erosion rate by landsliding in Amahata river basin, Japan. Z. Geomorphol., 29: 301–314.

Mietton, M., 1988. Dynamique de l'interface lithosphère–atmosphère en Burkina Faso. L'érosion en zone de savane. Thèse Doct. Univ. Grenoble I, 485 pp.

Moeyersons, J., 1981. Slumping and planar sliding on hill slopes in Rwanda. Earth Surf. Process., 6: 55–65.

Moeyersons, J., 1989. La nature de l'érosion des versants au Rwanda. Ann. R. Mus. Centr. Afr., Tervuren, Series Econ. Sc., 19, 396 pp.

Murray-Rust, D.H., 1972. Soil erosion and reservoir sedimentation in a grazing area west of Arusha, northern Tanzania. Geogr. Ann., 54A: 325–343.

Muxart, T., Cosandey, C., Billard, A. and Valdas, B., 1987. Dynamique des versants et occupation humaine dans les Cévennes (Montagne du Lingas). Bull. Ass. Géogr. Franç., 1: 1–40.

Nearing, M.A., Foster, G.R., Lane, L.J. and Finkner, S.C., 1989. A process-based soil erosion model for USDA-water erosion prediction project technology. Trans. ASAE, 32: 1587–1593.

Nordström, K., 1988. Gully erosion in the Lesotho lowland. Dept. of Phys. Geogr. Uppsala Univ., Ungi Rapport 69, 144 pp.

Olivry, J.C. and Hoorelbeck, J., 1990. Erodibilité des terres noires de la vallée du Buëch (France, Alpes du Sud). Cah. ORSTOM, Sér. Pédol., 25: 95–110.

Ollier, C.D. and Brown, M.J., 1971. Erosion of a young volcano in New Guinea. Z. Geomorphol. Suppl., 18: 12–28.

Osuji, G.E., 1984. The gullies of Imo. J. Soil Water Cons., 39: 246–247.

Pain, C.F. and Bowler, J.M., 1973. Denudation following the November 1970 earthquake at Madang, Papua-New Guinea. Z. Geomorphol. Suppl., 18: 92–104.

Panizza, M., 1990. The landslides in Cortina d'Ampezzo (Dolomites, Italy). In: Alpine Landslide Practical Seminar, 61th Int. Conf. and Field Workshop on Landslides, Switzerland, Austria, Italy, 79b, pp. 55–63.

Peyre, Y., 1990. Remembrement et lutte contre l'érosion dans le Département de l'Oise. ADEPRINA, Paris, 47 pp.

Piest, R.F., Bradford, J.M. and Wyatt, G.M., 1975. Soil erosion and sediment transport from gullies. J. Hydrol. Div., HY1: 65–80.

Pomeroy, J.S., 1980. Storm induced debris avalanching and related phenomena in the Johnstown area, Pennsylvania, with references to other studies in the Appalachians. U.S. Geol. Surv., Prof. Paper 1191.

Prior, D.B. and Douglas, G.R., 1971. Landslides near Larne, Coll. Antrim, 15–16th August 1970. Irish Geogr., 6: 294–301.

Rapp, A., 1972. Studies of soil erosion and sedimentation in Tanzania. Geogr. Ann., 54A: 105–379.

Rapp, A., 1974. Slope erosion due to extreme rainfall, with examples of tropical and arctic mountains. Abh. Akad. Wiss. Göttingen, Math.-Phys. Kl., 3F, 29: 118–136.

Renard, K.G., Foster, G.R. and Weesies, G.A. 1991. Predicting Soil Erosion by Water. A Guide to Conservation Planning with the Revised Universal Soil Loss Equation. USDA-ARS, Washington, DC.

Rice, R.M., Corbett, E.S. and Bailey, R.C., 1969. Soil slips, related to vegetation, topography and soil in Southern California. Water Resour. Res., 5: 647–659.

Richter, G., 1982. Quasinatürliche Hangformung in Rebsteilhängen und ihre Quantificierung: Das Beispiel Mertesdorfer Lorenzberg/Ruwertal. Z. Geomorphol., 43: 41–54.

Römkens, M.J.M., Prasad, S.N. and Poesen, J.W.A., 1987. Soil erodibility and properties. In: Trans. XII Congr. Int. Soc. Soil Sci., Hamburg, 1986, pp. 492–504.

Rossi, G. and Salomon, J.N., 1979. Un exemple d'érosion accélérée à Madagascar: les sakasaka. Z. Geomorphol., 23: 271–280.

Saunders, I. and Young, A., 1983. Rates of surface processes on slopes, slope retreat and denudation. Earth Surf. Process. Landforms, 8: 473–501.

Schumm, S.A., 1956. The role of creep and rainwash on the retreat of badland slopes. Am. J. Sci., 254: 693–706.

Selby, M.J., 1982. Hillslope Materials and Processes. Oxford University Press, Oxford, 264 pp.

Smith, B.J., 1982. Effects of climate and land-use changes on gully development: an example from Northern Nigeria. Z. Geomorphol. Suppl., 44: 33–51.

Sneddon, J., Williams, B.G., Savage, J.V. and Newman, C.T., 1988. Erosion of gully in duplex soils. Results of a long-term photogrammatric monitoring program. Aust. J. Soil Res., 26: 401–408.

Sutherland, R.A. and Bryan, R.B., 1991. Sediment budgeting: a case study in the Katiorin drainade basin, Kenya. Earth Surf. Process. Landforms, 16: 383–398.

Tang Keli, Xi Daoqing and Zang Pincang, 1987. The main types of soil erosion related to the characteristics of loess distribution: a representative basin of Xingzihe River. In: Liu Tungsheng (Editor), Aspects of Loess Research. China Ocean Press, Beijing, pp. 437–445.

Tijskens, E., 1988. Experimenten betreffende een model over de terugschrijding van geultrappen. M.Sc. Thesis, Katholieke Universiteit Leuven, 152 pp.

Van Noten, F. and De Ploey, J., 1977. Quaternary research in northeastern Nigeria. Ann. R. Mus. Centr. Afr. Tervuren, Hum. Sc., 92: 61 pp.

Wells, S.G., 1983. Regional badland development and a model of Late Quaternary evolution of badland watersheds, San Juan Basin, New Mexico. In: S.G. Wells, D.W. Love and T.W. Gardner (Editors), Field trip guidebook Conf. NW New Mexico, Am. Geom. Field Group, pp. 121–132.

Williams, M.A.J., 1973. The efficacy of creep and slope wash in tropical and temperate Australia. Aust. Geogr. Stud., 11: 62–78.

Wise, S.M., Thornes, J.B. and Gilman, A., 1982. How old are the badlands? A case study from south-east Spain. In: R. Bryan and A. Yair (Editors), Badland Geomorphology and Piping. Geo-Books, pp. 259–278.

Yair, A., 1974. Sources of runoff and sediment, supplied by the slopes of a first order drainage basin in an arid environment (Northern Negev, Israel). Abh. Ak. Wiss. Göttingen, 29: 403–417.

Zachar, D., 1982. Soil Erosion. Developments in Soil Science 10. Elsevier, Amsterdam, 547 pp.